

Catalytic Dehydrocoupling/Dehydrogenation of *N*-Methylamine-Borane and Ammonia-Borane: Synthesis and Characterization of High Molecular Weight Polyaminoboranes

Anne Staubitz,^{||†} Matthew E. Sloan,[†] Alasdair P. M. Robertson,[†] Anja Friedrich,[‡]
Sven Schneider,[‡] Paul J. Gates,[†] Jörn Schmedt auf der Günne,[§] and
Ian Manners^{*,†}

School of Chemistry, University of Bristol, Cantock's Close, Bristol, BS8 1TS, U.K., Technische Universität München, Department Chemie, Lichtenbergstraße 4, D-85747 Garching, Germany, and Department of Chemistry, Ludwig-Maximilians-Universität, Butenandtstr. 5-13, D-81377 Munich, Germany

Received May 27, 2010; E-mail: ian.manners@bristol.ac.uk

Abstract: The catalytic dehydrocoupling/dehydrogenation of *N*-methylamine-borane, MeNH₂·BH₃ (**7**), to yield the soluble, high molecular weight poly(*N*-methylaminoborane) (**8a**), [MeNH–BH₂]_n (*M_w* > 20 000), has been achieved at 20 °C using Brookhart's Ir(III) pincer complex IrH₂POCOP (**5**) (POCOP = [μ³-1,3-(OPtBu)₂C₆H₃]) as a catalyst. The analogous reaction with ammonia-borane, NH₃·BH₃ (**4**), gave an insoluble product, [NH₂–BH₂]_n (**8d**), but copolymerization with MeNH₂·BH₃ gave soluble random copolymers, [MeNH–BH₂]_{n-r}[NH₂–BH₂]_m (**8b** and **8c**). The structures of polyaminoborane **8a** and copolymers **8b** and **8c** were further analyzed by ultrahigh resolution electrospray mass spectrometry (ESI-MS), and **8a**, together with insoluble homopolymer **8d**, was also characterized by ¹¹B and ¹H solid-state NMR, IR, and wide-angle X-ray scattering (WAXS). The data indicate that **8a–8c** are essentially linear, high molecular weight materials and that the insoluble polyaminoborane **8d** possesses a similar structure but is of lower molecular weight (ca. 20 repeat units), presumably due to premature precipitation during its formation. The yield and molecular weight of polymer **8a** was found to be relatively robust toward the influence of different temperatures, solvents, and adduct concentrations, while higher catalyst loadings led to higher molecular weight materials. It was therefore unexpected that the polymerization of **7** using **5** was found to be a chain-growth rather than a step-growth process, where high molecular weights were already attained at about 40% conversion of **7**. The results obtained are consistent with a two stage polymerization mechanism where, first, the Ir catalyst **5** dehydrogenates **7** to afford the monomer MeNH=CH₂ and, second, the same catalyst effects the subsequent polymerization of this species. A wide range of other catalysts based on Ru, Rh, and Pd were also found to be effective for the transformation of **7** to polyaminoborane **8a**. For example, polyaminoborane **8a** was even isolated from the initial stage of the dehydrocoupling/dehydrogenation of **7** with [Rh(μ-Cl)(1,5-cod)]₂ (**2**) as the catalyst at 20 °C, a reaction reported to give the *N,N,N*-trimethyl borazine, [MeN–BH]₃, under different conditions (dimethoxyethane, 45 °C). The ability to use a variety of catalysts to prepare polyaminoboranes suggests that the synthetic strategy should be applicable to a broad range of amine-borane precursors and is a promising development for this new class of inorganic polymers.

Introduction

Polyolefins, [RCH–CH₂]_n, are arguably the most important synthetic polymers in modern day society with an annual market growth of 5–6%.¹ Their fundamental chemical and physical properties are well understood, and the current focus is on fine-tuning controlled polymerization techniques, to give access to tailor-made polymers in terms of tacticity and polydispersity index (PDI). The isoelectronic relationship between B–N and C–C bonds has played a well-recognized role in the teaching

and historical development of chemistry. Since the discovery of borazine, N₃B₃H₆, an “inorganic” analog of benzene in the 1920s,² this relationship has guided thinking about molecular BN species³ and also materials with 2D and 3D structures, such as hexagonal and cubic boron nitride (isoelectronic to graphite and diamond, respectively, with similar properties and applications).^{4,5} More recently, the BN/CC analogy has inspired the synthesis of a range of interesting new molecules and materials,

^{||} Present address: Otto Diels-Institut für Organische Chemie, Christian-Albrechts-Universität Kiel, Otto-Hahn-Platz 3, D-24118 Kiel, Germany.

[†] University of Bristol.

[‡] Technische Universität München.

[§] Ludwig-Maximilians-Universität.

(1) Kaminsky, W. *Macromol. Chem. Phys.* **2008**, *209*, 459.

(2) Stock, A.; Pohland, E. *Ber. Dtsch. Chem. Ges. B* **1926**, *59B*, 2215.

(3) Paetzold, P. *Adv. Inorg. Chem.* **1987**, *31*, 123.

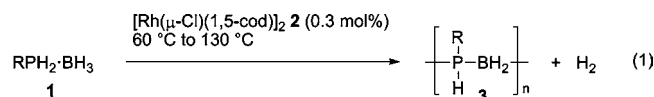
(4) Kaner, R. B.; Gilman, J. J.; Tolbert, S. H. *Science* **2005**, *308*, 1268.

(5) Pouch, J. J.; Alterovitz, S. A. *Synthesis and Properties of Boron Nitride (Materials Science Forum)*; Trans Tech Publications Ltd.: Zurich, 1990.

such as BN analogs of pyrene^{6–8} and carbon nanotubes⁹ as well as fullerene-like BN hollow spheres,¹⁰ and the fabrication of a highly ordered boron nitride nanomesh.¹¹ However, despite much effort in the 1950s and 1960s,¹² it was not possible to prepare and convincingly characterize high molecular weight, soluble polyaminoboranes [RNH–BH₂]_n, BN analogs of polyolefins.¹³ Well-characterized cycloliner polymers based on BN containing rings as the backbone have been shown to be useful preceramic materials^{14–17} and polymers with a cyclic B₂N₂-linker show promise as nonlinear optical materials.^{18–21} BN-linkages in the backbone have also been explored within the context of transition metal coordination polymers.^{22,23}

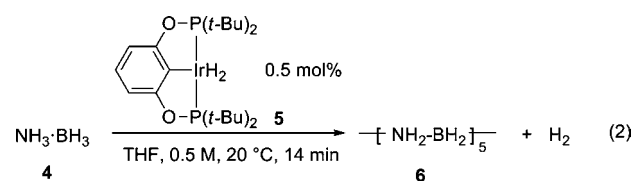
Catalytic dehydrogenation of primary amine-boranes and ammonia-borane^{24–48} offers a potential route to polyaminoboranes

analogous to the previously reported catalytic dehydrocoupling/dehydrogenation of primary phosphine-borane adducts (e.g., **1**). The latter have been shown to eliminate approximately 1 equiv of hydrogen with [Rh(μ -Cl)(1,5-cod)]₂ **2** as a catalyst, to yield high molecular weight polyphosphinoboranes [PhPH–BH₂]_n **3** (eq 1).^{49–53} However, in the studies reported to date for BN analogs, substantially more than 1 equiv of hydrogen is released to yield borazines and/or poorly characterized insoluble and branched oligomeric materials.^{24,27,30,37,38}



R = Ph, *i*-Bu, *p*-CF₃C₆H₄

The report by Goldberg, Heinekey and co-workers that Brookhart's IrH₂POCOP (**5**) catalyst⁵⁴ dehydrocouples NH₃·BH₃ (**4**) to yield the cyclic pentamer, [NH₂BH₂]₅ (**6**), with the elimination of 1 equiv of H₂³² (eq 2) inspired us to investigate the analogous chemistry with primary amine-borane adducts with the aim of preparing soluble polyaminoboranes.



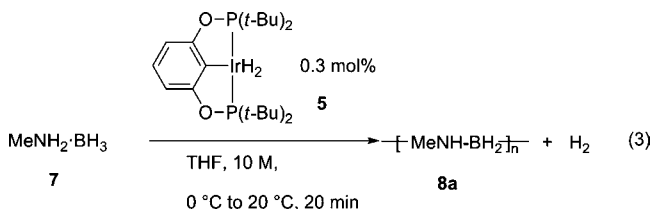
In a recent preliminary communication, we demonstrated the success of this approach and described the first well-character-

- (6) Liu, Z.; Marder, T. B. *Angew. Chem., Int. Ed.* **2008**, *47*, 242.
- (7) Piers, W. E.; Bosdet, M. J. D. *Can. J. Chem.* **2009**, *87*, 8.
- (8) Bosdet, M. J. D.; Piers, W. E.; Sorensen, T. S.; Parvez, M. *Angew. Chem., Int. Ed.* **2007**, *46*, 4940.
- (9) Terrones, M.; Romo-Herrera, J. M.; Cruz-Silva, E.; López-Urías, F.; Muñoz-Sandoval, E.; Velázquez-Salazar, J. J.; Terrones, H.; Bando, Y.; Golberg, D. *Mater. Today* **2007**, *10*, 30.
- (10) Wang, X.; Xie, Y.; Guo, Q. *Chem. Commun.* **2003**, 2688.
- (11) Corso, M.; Auwärter, W.; Muntwiler, M.; Tamai, A.; Greber, T.; Osterwalder, J. *Science* **2004**, *303*, 217.
- (12) Laubengayer, A. W. *Polymers - An International Symposium*; Chemistry Society: London, 1961; Vol. 15.
- (13) There have been attempts to synthesize in particular polyaminoborane [NH₂BH₂]_n by thermal reactions; the thermal decomposition of ammonia-borane: (a) Komm, R.; Geanangel, R. A.; Liepins, R. *Inorg. Chem.* **1983**, *22*, 1684. (b) Geanangel, R. A.; Rabalais, J. W. *Inorg. Chim. Acta* **1985**, *97*, 59. The thermal reaction of NaBH₄ and (NH₄)₂SO₄: (c) Kim, D.-P.; Moon, K.-T.; Kho, J.-G.; Economy, J.; Gervais, C.; Babonneau, F. *Polym. Adv. Technol.* **1999**, *10*, 702. The thermal decomposition of cyclotriborazane: (d) Baumann, J.; Baitalow, F.; Wolf, G. *Thermochim. Acta* **2005**, *430*, 9. Exposure of borazine to a radio frequency discharge: (e) Kwon, C. T.; McGee, H. A., Jr. *Inorg. Chem.* **1970**, *9*, 2458. But only insoluble products were obtained and the characterization was very limited. The only soluble polymer of this class that has been reported is poly(aminodifluoroborane) [NH₂BF₂]_n, for which no structural characterization was described but a molecular weight of 23 000 was claimed: (f) Pusatcioglu, S. Y.; McGee, H. A., Jr.; Fricke, A. L.; Hassler, J. C. *J. Appl. Polym. Sci.* **1977**, *21*, 1561.
- (14) Fazen, P. J.; Remsen, E. E.; Beck, J. S.; Carroll, P. J.; McGhie, A. R.; Sneddon, L. G. *Chem. Mater.* **1995**, *7*, 1942.
- (15) Fazen, P. J.; Beck, J. S.; Lynch, A. T.; Remsen, E. E.; Sneddon, L. G. *Chem. Mater.* **1990**, *2*, 96.
- (16) Wideman, T.; Sneddon, L. G. *Chem. Mater.* **1996**, *8*, 3.
- (17) Wideman, T.; Remsen, E. E.; Cortez, E.; Chlanda, V. L.; Sneddon, L. G. *Chem. Mater.* **1998**, *10*, 412.
- (18) Chujo, Y.; Tomita, I.; Murata, N.; Mauermann, H.; Saegusa, T. *Macromolecules* **1992**, *25*, 27.
- (19) Miyata, M.; Matsumi, N.; Chujo, Y. *Macromolecules* **2001**, *34*, 7331.
- (20) Matsumoto, F.; Chujo, Y. *Pure Appl. Chem.* **2006**, *78*, 1407.
- (21) A variety of polymers with boron in the main chain or side group structure have recently been reported. For example, see: (a) Lorbach, A.; Bolte, M.; Li, H.; Lerner, H.-W.; Holthausen, M. C.; Jäkle, F.; Wagner, M. *Angew. Chem., Int. Ed.* **2009**, *48*, 4584. (b) Malenfant, P. R. L.; Wan, J.; Taylor, S. T.; Manoharan, M. *Nat. Nanotechnol.* **2007**, *2*, 43–46. (c) Sundararaman, A.; Victor, M.; Varughese, R.; Jäkle, F. *J. Am. Chem. Soc.* **2005**, *127*, 13748. (d) Parab, K.; Venkatasubbaiah, K.; Jäkle, F. *J. Am. Chem. Soc.* **2006**, *128*, 12879. (e) Scheibitz, M.; Li, H.; Schnorr, J.; Sanchez Perucha, A.; Bolte, M.; Lerner, H.-W.; Jäkle, F.; Wagner, M. *J. Am. Chem. Soc.* **2009**, *131*, 16319.
- (22) Grosche, M.; Herdtweck, E.; Peters, F.; Wagner, M. *Organometallics* **1999**, *18*, 4669.
- (23) Dinnebie, R. E.; Wagner, M.; Peters, F.; Shankland, K.; David, W. I. F. *Z. Anorg. Allg. Chem.* **2000**, *626*, 1400.
- (24) Jaska, C. A.; Temple, K.; Lough, A. J.; Manners, I. *J. Am. Chem. Soc.* **2003**, *125*, 9424.
- (25) Conley, B. L.; Williams, T. J. *Chem. Commun.* **2010**, 4815.
- (26) Jiang, Y.; Blacque, O.; Fox, T.; Frech, C. M.; Berke, H. *Organometallics* **2009**, *28*, 5493.
- (27) Blaquiere, N.; Diallo-Garcia, S.; Gorelsky, S. I.; Black, D. A.; Fagnou, K. *J. Am. Chem. Soc.* **2008**, *130*, 14034.
- (28) Friedrich, A.; Drees, M.; Schneider, S. *Chem.—Eur. J.* **2009**, *15*, 10339.
- (29) Käss, M.; Friedrich, A.; Drees, M.; Schneider, S. *Angew. Chem., Int. Ed.* **2009**, *48*, 905.
- (30) Jaska, C. A.; Temple, K.; Lough, A. J.; Manners, I. *Chem. Commun.* **2001**, 962.
- (31) Chen, Y.; Fulton, J. L.; Linehan, J. C.; Autrey, T. *J. Am. Chem. Soc.* **2005**, *127*, 3254.
- (32) Denney, M. C.; Pons, V.; Hebden, T. J.; Heinekey, D. M.; Goldberg, K. I. *J. Am. Chem. Soc.* **2006**, *128*, 12048.
- (33) Fulton, J. L.; Linehan, J. C.; Autrey, T.; Balasubramanian, M.; Chen, Y.; Szymczak, N. K. *J. Am. Chem. Soc.* **2007**, *129*, 11936.
- (34) Douglas, T. M.; Chaplin, A. B.; Weller, A. S. *J. Am. Chem. Soc.* **2008**, *130*, 14432.
- (35) Sloan, M. E.; Clark, T. J.; Manners, I. *Inorg. Chem.* **2009**, *48*, 2429.
- (36) Rousseau, R.; Schenter, G. K.; Fulton, J. L.; Linehan, J. C.; Engelhard, M. H.; Autrey, T. *J. Am. Chem. Soc.* **2009**, *131*, 10516.
- (37) Keaton, R. J.; Blacquiere, J. M.; Baker, R. T. *J. Am. Chem. Soc.* **2007**, *129*, 1844.
- (38) Shrestha, R. P.; Diyabalanage, H. V. K.; Semelsberger, T. A.; Ott, K. C.; Burrell, A. K. *Int. J. Hydrogen Energy* **2009**, *34*, 2616.
- (39) Clark, T. J.; Russell, C. A.; Manners, I. *J. Am. Chem. Soc.* **2006**, *128*, 9582.
- (40) Pun, D.; Lobkovsky, E.; Chirik, P. J. *Chem. Commun.* **2007**, 3297.
- (41) Kawano, Y.; Uruichi, M.; Shimoi, M.; Taki, S.; Kawaguchi, T.; Kakizawa, T.; Ogino, H. *J. Am. Chem. Soc.* **2009**, *131*, 14946.
- (42) Hamilton, C. W.; Baker, R. T.; Staubit, A.; Manners, I. *Chem. Soc. Rev.* **2009**, *38*, 279.
- (43) Peng, B.; Chen, J. *Energy Environ. Sci.* **2008**, *1*, 479.
- (44) Marder, T. B. *Angew. Chem., Int. Ed.* **2007**, *46*, 8116.
- (45) Stephens, F. H.; Pons, V.; Baker, R. T. *Dalton Trans.* **2007**, 2613.
- (46) Clark, T. J.; Lee, K.; Manners, I. *Chem.—Eur. J.* **2006**, *12*, 8634.
- (47) Staubit, A.; Robertson, A. P. M.; Sloan, M. E.; Manners, I. *Chem. Rev.* **2010**, *110*, 4023.
- (48) Staubit, A.; Robertson, A. P. M.; Manners, I. *Chem. Rev.* **2010**, *110*, 4079.
- (49) Dorn, H.; Singh, R. A.; Massey, J. A.; Nelson, J. M.; Jaska, C. A.; Lough, A. J.; Manners, I. *J. Am. Chem. Soc.* **2000**, *122*, 6669.
- (50) Dorn, H.; Singh, R. A.; Massey, J. A.; Lough, A. J.; Manners, I. *Angew. Chem., Int. Ed.* **1999**, *38*, 3321.

ized high molecular weight, soluble polyaminoboranes from readily available amine-borane adduct precursors such as $\text{MeNH}_2 \cdot \text{BH}_3$ (**7**) at ambient temperature.^{55–57} The analogous formation of oligomers (up to a molecular weight of ca. 2000) rather than high molecular weight polymers from **7** was reported independently shortly thereafter by Goldberg and Heinekey.⁵⁸ In this paper we report a detailed study and further development of a selection of this work, with a focus on the dehydropolymerization and dehydrocopolymers of **7** and **4**.

Results

(1) Catalytic Dehydrogenation of $\text{MeNH}_2 \cdot \text{BH}_3$ and $\text{NH}_3 \cdot \text{BH}_3$ by IrH_2POCOP (5**). (a) Synthesis and Characterization of the Homopolymer $[\text{MeNH}-\text{BH}_2]_n$ (**8a**).** Based on the observation by Goldberg and Heinekey that IrH_2POCOP (**5**) released *only* 1 equiv of hydrogen from ammonia-borane³² we explored the use of *N*-methylamine-borane **7** as a monomer with the aim that the methyl group would serve as a solubilizing side chain. When a concentrated solution of **7** in THF (10 M) was treated with **5** (0.3 mol % at 0 °C), we observed vigorous bubbling and a rapid increase of the viscosity of the reaction mixture. After about 1 min, the mixture was allowed to stir at 20 °C for 20 min (eq 3). Subsequently, the polymer could be easily purified by precipitation into alkanes as nonsolvents to give **8a** as an off-white solid in high yield (60%).



Polymer characterization was performed by NMR spectroscopy (¹H, ¹¹B, and ¹³C; for the spectra see Figures SI 1 and SI 2), infrared spectroscopy (IR; for the spectra see Figure SI 3), elemental analysis (EA), and wide-angle X-ray scattering (WAXS) (Figure SI 4 and Table SI 1). For an estimation of the molecular weight we used gel permeation chromatography (GPC; for the trace see Figure SI 5). The polymers were further analyzed by thermogravimetric analysis (TGA) (Figure SI 6) and dynamic light scattering (DLS) (Figures SI 7 and 8, Tables SI 2a–d).⁵⁹ Analysis by ¹¹B{¹H} NMR spectroscopy (in CDCl₃) gave a broad peak at –6.5 ppm, which did not resolve into a triplet in the proton coupled ¹¹B NMR spectrum. This effect may be due to a range of slightly different magnetic environments for boron (arising from proximity to the middle or end of the polymer chain or different tactic environments), fast relaxation, and/or the influence of restricted rotation. Significantly, the chemical shift for the ¹¹B NMR peak for

8a (–6.5 ppm) is similar to that for both isomers of the analogous borazane six-membered ring $[\text{MeNH}-\text{BH}_2]_3$ ($\delta = -5.4$ ppm in acetone-*d*₆).⁶⁰ In the case of this small molecule species, coupling to hydrogen was detected in the proton-coupled ¹¹B NMR spectrum (¹J_{BH} = 107 Hz). The ¹H NMR spectrum of **8a** in CDCl₃ showed a signal at $\delta = 2.75$ ppm for the protic hydrogen on nitrogen, a broad peak with at least one shoulder for the methyl group at 2.18 ppm and another broad peak centered at 1.68 ppm for the hydridic hydrogens on boron. The line shape of the methyl group may arise from different tactic environments but was not well resolved enough to attempt a meaningful deconvolution of the peak. In the ¹³C NMR spectrum, the different tactic environments for the methyl group were better resolved and gave two discernible peaks at $\delta = 36.9$ (br) and 35.9 ppm, but the deconvolution of the line shape led us to suspect that they are comprised of a series of peaks with similar chemical shifts. The IR spectrum of **8a** proved useful for structural characterization (Figure SI 3) and showed a high frequency band at $\tilde{\nu} = 3256$ cm^{–1}, characteristic for N–H vibrations, a band at 2985 cm^{–1} for the C–H stretches in the methyl group, and a band at 2366 cm^{–1} for the B–H stretching mode. The elemental analysis was correct if residual THF (as quantified by ¹H NMR spectroscopy) was taken into account.^{59,61} The solvent appeared so tightly bound in the polymer matrix that even precipitation from THF into a nonsolvent could not remove it completely, which attests to the polar nature of **8a**. Only when the polymer was precipitated twice from dichloromethane into *n*-butane could the THF be removed completely, but the solubility of the polymer decreased sharply and CH₂Cl₂ was retained instead (for further information see Figure SI 2).

GPC analysis of **8a** in THF containing 0.1 w/w% *n*-Bu₄NBr showed a relatively broad peak (PDI = 2.9) corresponding to a polymer with an estimated weight average molecular weight (*M*_w) of 160 000, relative to polystyrene standards.⁶² DLS measurements (in pure THF) gave a hydrodynamic radius (*R*_H) of ca. 3 nm, a value typical for a macromolecular species in solution.⁶³ For comparison, poly(2-ethyl-2-oxazoline), a polymer likely to possess a much more similar polarity to **8a** than polystyrene, an *R*_H value of 3 nm in pure THF corresponds to an *M*_w value of ca. 50 000.^{63b} We also compared the DLS and GPC data for the sample of **8a** to narrow molecular weight distribution samples of poly(methylmethacrylate) (PMMA), another polar organic polymer. This indicated an *M*_w value of

- (51) Dorn, H.; Rodezno, J. M.; Brunnhofer, B.; Rivard, E.; Massey, J. A.; Manners, I. *Macromolecules* **2003**, *36*, 291.
 (52) Clark, T. J.; Rodezno, J. M.; Clendenning, S. B.; Aouba, S.; Brodersen, P. M.; Lough, A. J.; Ruda, H. E.; Manners, I. *Chem.—Eur. J.* **2005**, *11*, 4526.
 (53) Denis, J. M.; Forintos, H.; Szelke, H.; Toupet, L.; Pham, T. N.; Madec, P. J.; Gaumont, A.-C. *Chem. Commun.* **2003**, 54.
 (54) Göttker-Schnetmann, I.; White, P.; Brookhart, M. *J. Am. Chem. Soc.* **2004**, *126*, 1804.
 (55) Staubitz, A.; Soto, A. P.; Manners, I. *Angew. Chem., Int. Ed.* **2008**, *47*, 6212.
 (56) Pons, V.; Baker, R. T. *Angew. Chem., Int. Ed.* **2008**, *47*, 9600.
 (57) Ihara, E. *Organomet. News* **2009**, 26.
 (58) Dietrich, B. L.; Goldberg, K. I.; Heinekey, D. M.; Autrey, T.; Linehan, J. C. *Inorg. Chem.* **2008**, *47*, 8583.

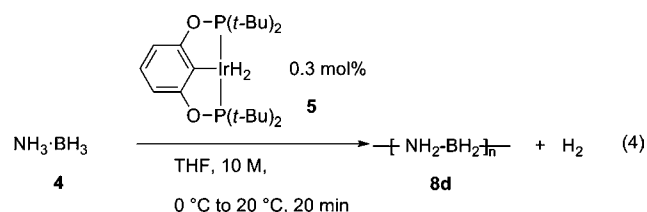
- (59) When polymerization reactions are performed in THF, the potential formation of poly(THF) always needs to be considered as this material could be mistaken for the desired polymer in GPC experiments. Careful inspection of the ¹H NMR spectra indicated that this was not the case: poly(THF) in CDCl₃ has ¹H NMR data as follows: $\delta = 1.53$ – 1.69 (m) and 3.31 – 3.55 (m) ppm (see: Tezuka, Y.; Tsuchitani, A.; Oike, H. *Macromol. Rapid Commun.* **2004**, *25*, 1531) whereas the signals of molecular THF appear downfield $\delta = 1.85$ (m) and 3.76 (m) ppm (see: Gottlieb, H. E.; Kotlyar, V.; Nudelman, A. *J. Org. Chem.* **1997**, *62*, 7512. In the ¹H NMR spectra for polymer **8a** in CDCl₃ resonances were detected at $\delta = 1.82$ (m) and $\delta = 3.72$ (m) ppm consistent with the presence of molecular THF (see Figure SI 1). It should also be noted that polyaminoborane **8a** free of THF was prepared which indicated that it is not part of the polymer structure (see Figure SI 2).
 (60) Narula, C. K.; Janik, J. F.; Duesler, E. N.; Paine, R. T.; Schaeffer, R. *Inorg. Chem.* **1986**, *25*, 3346.
 (61) This particular sample had been precipitated into *n*-butane, which was also present, but in negligible amounts.
 (62) In pure THF the GPC traces for polymer **8a** showed evidence for significant column adsorption effects with an observable tail to lower molecular weight (see Figure SI 8a). The addition of *n*-Bu₄NBr was used to increase the ionic strength of the solution for polar polyaminoboranes **8a**–**8c** and led to much better defined GPC traces (see Figure SI 7a).

at least 23 000 for a sample of **8a** with $R_H = 3$ nm in THF. These results suggest that GPC analysis in THF containing 0.1 w/w% *n*-Bu₄NBr using polystyrene standards for column calibration may overestimate the molecular weight (M_w) of this sample of **8a** by a factor of approximately up to 3 to 6. Bearing this in mind, approximate weight average degrees of polymerization (DP_w) and number average degrees of polymerization (DP_n) for **8a** for this sample are at least 600 and 200, respectively.

A series of additional GPC and DLS experiments were performed to further confirm the macromolecular nature of **8a**. In order to exclude the presence of aggregates rather than true macromolecules in solution, we explored the potential variation of the molecular weight, PDI, and hydrodynamic radius (R_H) with concentration (from 0.4 to 4 mg/mL) for a sample of **8a**. If the GPC or DLS peak were due to aggregates, a distinct dependence of these parameters on concentration would be anticipated.⁶⁴ Thus, higher concentrations should lead to larger aggregates and to shorter retention times by GPC and larger hydrodynamic radii by DLS. However, this was not observed experimentally, and instead, the GPC and DLS peaks had the same retention times within experimental error, irrespective of the concentration. This confirmed the presence of discrete macromolecules in solution.

By WAXS, polymer **8a** prepared with IrH₂POCOP **5** appeared completely amorphous (Figure SI 4). Thermogravimetric analysis at a heating rate of 10 °C/min showed a decomposition temperature of ca. 180 °C with an inflection point of ca. 160 °C with a ceramic yield of 25% at 600 °C (Figure SI 6a).

(b) **Synthesis and Characterization of Polyaminoborane [NH₂-BH₂]_n (**8d**) and Random Copolymers [NH₂-BH₂]_m-r-[MeNH-BH₂]_n (**8b** and **8c**).** The catalytic dehydrocoupling reaction of ammonia-borane (**4**) with Ir catalyst **5** gave a white solid product (**8d**),⁵⁵ which was insoluble in alkanes, benzene, toluene, alcohols, THF, dioxane, pyridine, DMF, DMSO, water, or acetonitrile (eq 4).



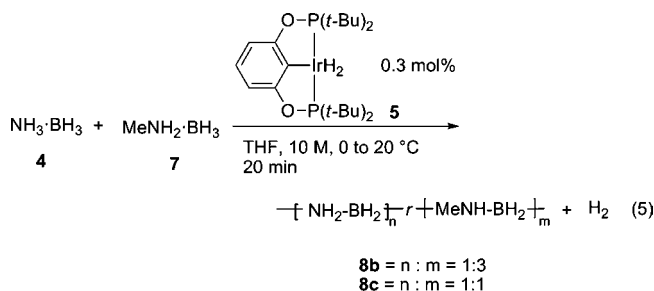
While this fact simplified purification by filtration and washing of the filtrate with THF, analysis of this product was impeded and we could only employ solid state techniques. The IR spectrum (Figure SI 3) was particularly insightful. Two sharp bands at 3299 and 3248 cm⁻¹ were observed, which we assigned to the asymmetric and symmetric N-H stretches, respectively.

(63) Macromolecules typically possess R_H values significantly larger than 1 nm in solution. As pure THF is anticipated to be a thermodynamically poor solvent for highly polar polyaminoboranes such as **8a**–**8c**, the polymer coils would be expected to be in a contracted state in this solvent. Thus the R_H value is likely to be substantially lower than for less polar polymers of comparable molecular weight for which THF is a thermodynamically good solvent. For example, for non-polar polystyrene, $R_H = \text{ca. } 3$ nm corresponds to $M_w = \text{ca. } 20\,000$ in THF. (a) Mandema, W.; Zeldenrust, H. *Polymer* **1977**, *18*, 835. In comparison, for a polar polymer such as poly(2-ethyl-2-oxazoline), $R_H = \text{ca. } 3$ nm corresponds to a M_w value of ca. 50 000 in THF; (b) Sung, J. H.; Lee, D. C. *Polymer* **2001**, *42*, 5771.

(64) Solc, K.; Elias, H. G. *J. Polym. Sci., Polym. Phys. Ed.* **1973**, *11*, 137.

A broader, less well resolved peak with a sharp feature at 2356 cm⁻¹ was assigned for the corresponding B–H modes. This spectrum differed significantly from that observed by Kim and co-workers for a material which they had obtained in low yield from the thermal reaction of NaBH₄ and (NH₄)₂SO₄.^{13c} In their spectrum, the N–H bands were much less defined and flanked by a substantial broad shoulder toward higher wavenumbers. Likewise, the B–H stretching vibrations appeared as a single broad band, without any underlying multipeak structure. The IR spectrum of **8d** also differed from other samples reported to be polyaminoborane, [NH₂-BH₂]_n, which had been prepared by subjecting borazine to a radio frequency discharge (by McGee Jr. and co-workers),^{13e} by thermal decomposition of cyclotriborazane (Baumann and co-workers),^{13d} or by thermal decomposition of ammonia-borane (Geangel and Liepins),^{13a} which all showed less defined, broader peaks at slightly different wavenumbers. WAXS data for **8d** showed a sharp peak, suggesting a semicrystalline material (Figure SI 4). Comparison to the X-ray diffraction pattern with the isoelectronic polyethylene (ca. $2\theta = 21^\circ$, d -spacing 4.2 Å) in its semicrystalline state⁶⁵ revealed a smaller unit cell for **8d** ($2\theta = 23.25^\circ$, d -spacing 3.8 Å). These results also differed substantially from those reported earlier for materials reported to be polyaminoborane [NH₂-BH₂]_n: samples prepared by Kim^{13c} or Baumann^{13d} appeared amorphous, whereas the material prepared by Geangel and Liepins appeared semicrystalline,^{13a} but with d -spacings that differ from those we determined for **8d**. TGA analysis for this material gave a ceramic yield of 40 wt % at 600 °C (Figure SI 6b) with a decomposition temperature of ca. 220 °C (inflection point ca. 200 °C), which also differed from the other materials reported as polyaminoborane, which were around 75–80% at 1000,^{13c} 480,^{13d} and 500 °C,^{13f} regardless of the preparation used.^{13c,d,f} Elemental analysis of **8d** revealed some carbon was present that presumably originated from residual solvent, which could not be removed despite applying high vacuum (ca. 10⁻³ mbar) to the sample. Further characterization of **8d** by solid state NMR was exceptionally useful and is discussed in section 3b (ii) below.

We hypothesized that copolymerization of NH₃·BH₃ (**4**) with the *N*-methylamine-borane adduct **7** might yield soluble random copolymers (eq 5). When a mixture of **4** and **7** in a ratio of 1:3 in THF (10 M) was reacted with 0.3 mol % of **5**, vigorous bubbling ensued and the yellow reaction mixture became very viscous. Copolymer (**8b**) was then isolated as a white solid by precipitation into *n*-alkanes as nonsolvent (Table 1, entry 2). When the ratio was further reduced to 1:1, the same vigorous H₂ evolution was observed, but the resulting solution was no longer clear (Table 1, entry 3). The increased insolubility was reflected by the increased isolated yield of copolymer **8c** after precipitation (eq 5).



GPC confirmed the macromolecular nature of **8b**. It was also possible to obtain a GPC trace of polymer **8c** in THF containing

(65) Krimm, S. *J. Phys. Chem.* **1953**, *57*, 22.

Table 1. Synthesis and Molecular Weight Data for Polyaminoboranes **8a–8d**

Entry	Monomer precursors (ratio)	polyaminoborane	Isolated yield ^a / %	M_w (PDI) (GPC)	R_H^b / nm (DLS)
1	MeNH ₂ ·BH ₃	[MeNH–BH ₂] _n (8a)	60	160 000 (2.9)	3 ^c
2	MeNH ₂ ·BH ₃ / NH ₃ ·BH ₃ (3: 1)	[MeNH–BH ₂] _{3<i>n</i>-<i>r</i>}	72	156 000 (11.0)	3 ^c
3	MeNH ₂ ·BH ₃ / NH ₃ ·BH ₃ (1: 1)	[NH ₂ –BH ₂] _n (8b)	91	47 000 (3.9)	4 ^d
4	MeNH ₂ ·BH ₃ / NH ₃ ·BH ₃	[MeNH–BH ₂] _{n-<i>r</i>} [NH ₂ –BH ₂] _n (8c) [NH ₂ –BH ₂] _n (8d)	98	<i>e</i>	<i>e</i>

^a The reaction (in THF, ca. 0.3 mol % **5**, 20 min) is quantitative by ¹¹B NMR. ^b R_H = hydrodynamic radius by Dynamic Light Scattering. ^c In THF. ^d In DMSO. ^e Not determined; insoluble product.

0.1 w/w% *n*-Bu₄NBr, but the sample did not dissolve completely and it is likely that higher molecular weight fractions of the copolymer were retained by the filtration of the sample before injection. DLS analysis of **8c** could not be performed in THF due to the low solubility but was performed in DMSO where the solubility was higher and an R_H value of 4 nm was determined. By ¹¹B NMR spectroscopy (1:1 CDCl₃/DMSO-*d*₆), both copolymers **8b** and **8c** showed a featureless broad peak at –9.0 and –11.0 ppm, respectively. In the ¹H NMR spectra of **8b** and **8c** (in CDCl₃) only very broad peaks were detected, which showed the signals for N–H, Me, and BH groups in the expected region. While the integration matched the expected ratio of the peaks based on the monomer feed ratio, more decisive evidence for the incorporation of the NH₂–BH₂ unit into the copolymer was desirable. This was obtained by the analysis of copolymers **8b** and **8c** by ESI-MS where series of peaks were observed that showed both a mass difference of 29.04 for the [NH₂–BH₂] fragment and 43.06 for the [MeNH–BH₂] fragments (see section 3a (i) and Figures SI 9 and SI 10).

(2) Detailed Studies of the Catalytic Dehydrogenation of MeNH₂·BH₃ with IrH₂POCOP (5**).** **(a) Recycling of the IrH₂POCOP Catalyst.** The ability to recycle the Ir(III) catalyst was examined by allowing a polymerization of **7** to proceed for 1 h followed by precipitation and isolation of polymer **8a** under anaerobic and anhydrous conditions. Removal of the solvent from the supernatant left a brown residue, which on dissolution in THF was added to another batch of **7**, dissolved in THF. The reaction proceeded immediately with vigorous H₂ evolution. This procedure was repeated a further time. GPC traces of these reactions (see Figure SI 11, Table SI 3) showed that the first two polymerizations gave polymer **8a** of similar molecular weight (Run 1: M_w = 141 300, PDI = 2.7, Run 2: M_w = 121 300, PDI = 2.3). The last batch showed a molecular weight of M_w = 86 000 (PDI = 2.4). Bearing in mind the possible loss of **5** during isolation and the substantial polydispersities of the samples, the results are consistent with no significant changes in molecular weight on recycling of the Ir catalyst.

(b) Influence of Substrate Concentration and Catalyst Loading on Molecular Weight. We first performed reactions at concentrations of substrate **7** ranging from 0.5 to 10 M with a catalyst loading of 0.1 mol % and found that all reactions gave high molecular weight polymers by GPC, ranging from M_w = 95 000 to 226 000, PDI 2.6 to 3.7 (see Table SI 4, entries 1–8). Under these conditions the molecular weights did not vary more than within experimental error, except for the reaction at highest dilution (0.5 M), where the molecular weight was slightly reduced (M_w = 95 000; PDI = 3.9; for comparison, the weight average molecular weight was M_w = 165 000; PDI = 2.6 for

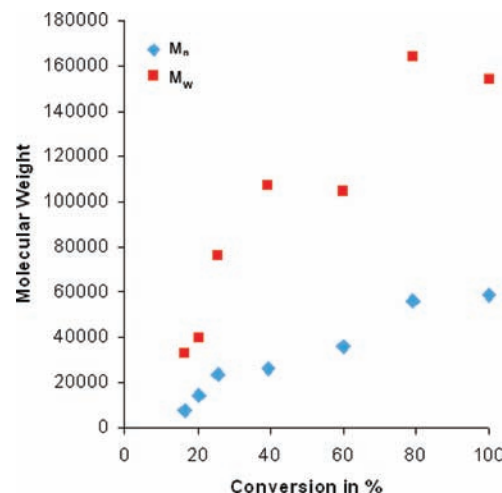


Figure 1. Molecular weight (M_n and M_w) versus conversion plot for the formation of poly(*N*-methylaminoborane) **8a** from **7** using Ir catalyst **5** (0.1 mol % **5**, THF, 0.5 M in **8a**, 20 °C). The point at ca. 40% conversion represents the average of two individual runs (run 1: M_w = 125 500, M_n = 33 600, run 2: M_w = 88 300, M_n = 19 000).

a 2 M reaction).⁶⁶ A second series of experiments was then conducted where the substrate concentration was kept at 2 M and the catalyst loading was varied from 6.6 mol % to 0.05 mol %. We found that under all of these conditions a high molecular weight polymer was formed by GPC analysis. As a general trend, higher catalyst loadings led to higher molecular weights (up to M_w = 356 000 with PDI = 3.1 with 6.6 mol % of **5**), irrespective of the concentration (for individual results, see Table SI 4, entries 9–13; also compare entries 1 and 14).

(c) Mechanism of the Polymerization: Chain Growth versus Step Growth. The distinction between a step-growth and a chain-growth process is a fundamental aspect of polymerization mechanistic analysis. In a step-growth mechanism monomers and oligomers can react with one another at similar rates. In such a process, long chain polymers appear only at high monomer conversion. By contrast, chain-growth mechanisms are characterized by the formation of a high molecular weight polymer at low monomer conversion. In order to ascertain which type of mechanistic behavior is present with **5** as the catalyst, we monitored a reaction of **7** (0.5 M, THF) with a catalyst loading of 0.1 mol % (Figure 1).

The reaction was monitored in a closed system with a manometer (Figures SI 12 and SI 13).⁶⁶ Because of this

(66) We estimate that the numerical error for M_w is around 5%, whereas for M_n it is mostly around 10%, except for samples with a broad distribution, where we see errors up to 20%.

(67) The polymerization reaction was very rapid and difficult to follow by NMR spectroscopy due to a hydrogen pressure buildup.

experimental setup, every point in the plot was taken from a separate reaction, where each reaction was allowed to proceed to the desired conversion based on the average measured pressure at 100% conversion (equal to 1 equiv of released hydrogen). For the estimation of the molecular weight, this mixture was then precipitated into hexane at $-78\text{ }^{\circ}\text{C}$, and the precipitated polyaminoborane **8a** was filtered off and analyzed by GPC. Significantly, the molecular weight at 100% conversion was the same as that in the open system, which demonstrated that the gradual buildup of hydrogen had no appreciable influence on this parameter.⁶⁸

The polydispersity of the samples of polyaminoborane **8a** was between 2.6 and 4.6, and although it was difficult to ascertain the low end of the GPC trace due to tailing effects, the overall trend was still clearly visible. The M_n and M_w versus conversion plot showed that high molecular weight polymers were present even at low conversion (<40%), confirming the chain growth character of the polymerization. However, the chain length increased at higher conversion. This indicated that the polymerization differs from classical chain growth polymerizations such as radical polymerization, where a high molecular weight polymer is formed at very low conversion but no further significant increase in chain length is detected with higher conversion.⁶⁹

(d) Variation of Solvents and Temperature. We also investigated whether the polymerization proceeded in solvents other than THF. Reactions performed in dioxane, diethyl ether, and toluene (20 $^{\circ}\text{C}$, 0.5 M, 20 h, 0.1 mol % of Ir catalyst **5**) all gave a high molecular weight polymer (see Table SI 5). The solubility of **8a** in dioxane and diethyl ether was limited, and precipitation occurred; however removal of the reaction solvent and analysis of the product by GPC upon dissolution in THF (0.1 w/w% *n*-Bu₄NBr) showed no reduction in molecular weight. In the case of toluene, the starting material was only partially soluble, and some starting material remained after 20 h, but the molecular weight appeared not to be diminished upon analysis by GPC.

Linear poly(*P*-phenylphosphinoborane) can be lightly cross-linked at elevated temperatures in the presence of Rh catalysts to give swellable gels.⁴⁹ We therefore investigated whether a similar process was also possible with poly(*N*-methylaminoborane). Catalytic dehydropolymerization reactions of **7** were performed at 40 and 60 $^{\circ}\text{C}$ in THF (10 M) with **5** (0.3 mol %) for 1 h. No evidence of cross-linking was observed; the polymers were still completely soluble and were of high molecular weight and possessed similar molecular weight distributions to that formed at 20 $^{\circ}\text{C}$ (by GPC, Table SI 6).⁷⁰

(3) Further Structural Characterization of the Homopolymer Poly(*N*-methylaminoborane) (8a**), Random Copolymers (**8b** and **8c**) and Polyaminoborane **8d**.** **(a) Structural Analysis by Mass Spectrometry.** **(i) Electrospray Ionization Mass Spectrometry (ESI-MS).** A sample of high molecular weight polyaminoborane **8a** ($M_w = 214\,000$, PDI = 2.0 by GPC) prepared using a catalyst loading of 0.3 mol % of **5** was analyzed by ESI-MS, in both positive and negative ionization modes using a range of different cone potentials.⁷¹ Close inspection of the ESI-MS spectrum (positive mode, +150 V cone potential, Figure SI 14) of **8a**

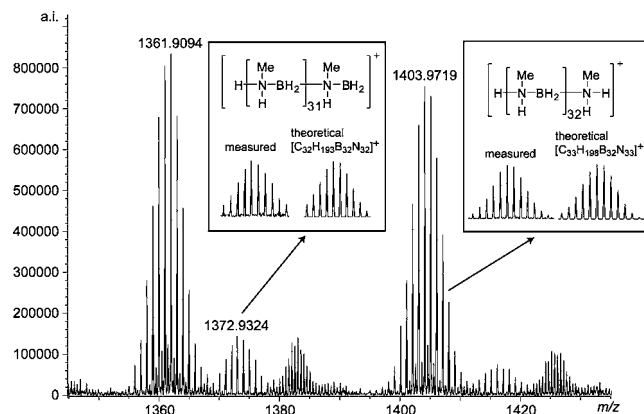


Figure 2. Poly(*N*-methylaminoborane) **8a** in ESI-MS at +150 V, positive mode; measured and calculated isotope distribution. Catalyst: IrH₂POCOP (**5**). $M_w = 214\,000$, PDI = 2.0 by GPC (THF, 0.1 w/w% *n*-Bu₄NBr). Also visible are a series of peaks with very narrowly spaced lines which indicate the presence of doubly charged species ($z = 2$).

revealed the presence of two series of peaks, one of a higher intensity corresponding to linear species $[\text{H}-(\text{NMeH}-\text{BH}_2)_n-\text{NMeH}_2]^+$ with the maximum of the peak distribution at approximately 1061 m/z and a lower intensity series with the maximum of the peak distribution at approximately 516 m/z corresponding to the linear species losing a hydride $[\text{H}-(\text{MeNH}-\text{BH}_2)_n]^+$ (see Figure 2 for an expansion of a representative section). The maximum observed mass was around 3000 m/z , corresponding to a degree of polymerization of about 70. When we varied the cone potential, the observed distributions changed. For example, at +350 V (a much higher value than normally used) the maximum of the peak distribution for $[\text{H}-(\text{NMeH}-\text{BH}_2)_n-\text{NMeH}_2]^+$ shifted to approximately 1834 m/z with peaks again detected to roughly 3000 m/z (Figure SI 15). The molecular weights indicated by ESI, which from the maxima at 1061–1834 m/z already correspond to ca. 25–42 repeat units, are nevertheless far below that indicated by GPC for this sample of **8a** ($M_w = 214\,000$, PDI = 2.0 in THF containing 0.1 w/w% *n*-Bu₄NBr). Significantly, the hydrodynamic size indicated by DLS measurements ($R_H = \text{ca. } 3.2\text{ nm}$ in pure THF) is also indicative of a polymeric rather than an oligomeric material of molecular weight <3000.^{63,72} These observations suggest that ESI-MS does not allow a realistic estimation of the molecular weight of polyaminoborane **8a**.

In negative ion mode two distributions were detected, one corresponding to $[\text{H}_3\text{B}-(\text{NMeH}-\text{BH}_2)_n-\text{H}]^-$ and another of much lower intensity. This lower intensity distribution could correspond to a polymer where a proton has been replaced with a sodium ion, $[\text{NaH}_2\text{B}(\text{NMeH}-\text{BH}_2)_n-\text{H}]^-$, but the low signal-

(68) A precipitation step might be expected to alter the molecular weight distribution of a polymer sample. However, we found that the shape and retention time of the GPC peaks from samples before and after precipitation were identical within experimental error.

(69) Odian, G. *Principles of Polymerization*; John Wiley & Sons, Inc.: NJ, 2004.

(70) The Ru complex **12** (Table 2, entry 4) is stable in DMSO at room temperature, possibly allowing for heating the reaction to higher temperatures. However, the reactions (0.1 mol% catalyst, 10 M) were less clean. At 20 $^{\circ}\text{C}$, the reaction was complete after 45 minutes with a major, sharp peak (<98%) in the ¹¹B NMR spectrum at -6.0 ppm . No high molecular weight polymer was detected by GPC for this reaction, only peaks for low molecular weight products. At 60 $^{\circ}\text{C}$ after 45 min, a considerable amount of starting material (**7**) (ca. 50%) was still present in the reaction mixture suggesting that the catalyst species was rapidly deactivated under these conditions. For catalyst deactivation using **12**, see reference 28.

(71) A detailed report including the ESI-MS data of the polymers formed by the non-Ir catalysts will be published at a later stage.

(72) For poly(2-ethyl-2-oxazoline) $R_H = 2\text{ nm}$ in THF corresponds to an M_w value of ca. 20 000. See ref 63 and references cited therein for further discussions.

to-noise ratio made it impossible to confirm the theoretical isotope pattern (see Figure SI 16).

ESI-MS was also used to analyze the copolymers **8b** and **8c** formed by the Ir-catalyzed dehydropolymerization of **4** and **7**. The quality of the spectrum for **8c** was relatively poor, which we attribute to the poor solubility and the low volatility of this material in the spectrometer. However, for **8b**, at a positive cone potential of +150 V, a broad distribution was observed, with a maximum of 933, which corresponds to an average degree of polymerization of 24 up to a mass range of about 2400, corresponding to ca. 62 repeat units (if a weighted mass average of 39 is used for the monomer) (Figure SI 9). Closer inspection of the individual peaks revealed monomer unit mass differences of 29 and 43, corresponding to $-\text{[NH}_2\text{-BH}_2\text{]}-$ and $-\text{[MeNH-BH}_2\text{]}-$ repeat units, respectively (Figure SI 10). However, due to overlying mass distributions, a comparison between experiment and calculated isotope distributions was not possible. These results suggest that the unsubstituted polyaminoborane **8d** is likely to be also a linear polymer which, due to strong inter- and intramolecular dihydrogen bonds, is insoluble in common organic solvents.

(ii) Nanospray Mass Spectrometry. In the ESI-MS ionization source⁷³ the sample solution is heated to 200 °C by the nitrogen drying gas, which could contribute to the fragmentation of the polymer. Nanospray^{74,75} on the other hand, which is a variant of conventional ESI-MS, does not require heating of the sample solution, because low injection flow rates allow for much more efficient desolvation to occur at room temperature when compared to conventional ESI-MS. However, because nanospray is essentially the same ionization technique, the results can be compared in order to try to eliminate ionization artifacts. There has been some debate in the literature about the differences between nanospray and ESI-MS. Certainly highly conjugated (and aromatic) species appear to ionize slightly differently.^{76,77} However, with polyaminoboranes, which do not possess π -conjugation, this is unlikely to be an issue. For **8a**, as with ESI-MS, using nanospray we observed up to three different distributions in both positive and negative ionization modes, the maxima of which shifted as different voltages were applied. In positive ionization mode (+125 V), the distribution with the maximum at highest molecular weight ($m/z = 933$) corresponded to $[\text{H}-(\text{NMeH-BH}_2)_n-\text{NMeH}_2]^+$ ($n = 21$) and a lower molecular weight distribution with a maximum corresponding to $[\text{H}(\text{NMeH-BH}_2)_n]^+$ ($n = 7$) was also detected (Figure 3).⁷⁸

In the negative mode two distributions were observed, whose maxima were dependent on the applied voltage. At -125 V, the more intense peaks could be assigned to the series $[\text{H}_3\text{B}-(\text{NMeH-BH}_2)_n-\text{H}]^-$ with a maximum at 915 m/z , corresponding to a DP_N of 22 (Figure SI 18). Similarly to ESI-MS, the weaker distribution could correspond to a polymer where a proton has been replaced with a sodium ion,

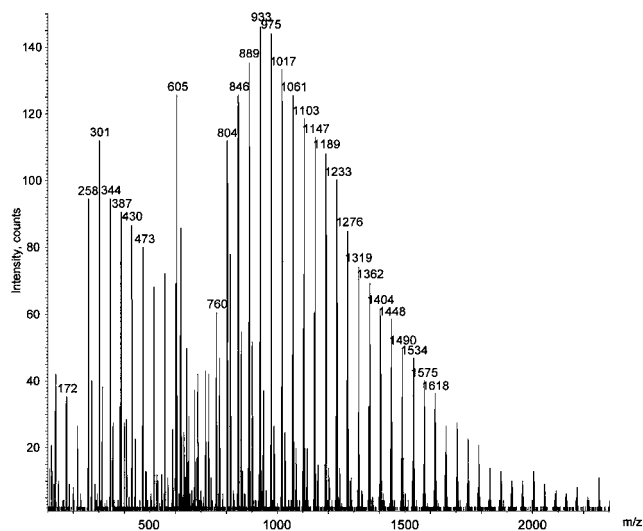


Figure 3. Poly(*N*-methylaminoborane) **8a** by nanospray MS at +125 V, positive mode. Catalyst $\text{IrH}_2\text{POCOP } 5$. $M_w = 214\,000$, PDI = 2.0 by GPC (THF, 0.1 w/w% *n*-Bu₄NBr).

$[\text{NaH}_2\text{B}-(\text{NMeH-BH}_2)_n\text{H}]^-$, but the low resolution of the nanospray spectrum made it impossible to confirm with a theoretical isotope pattern.

A comparison between ESI-MS and nanospray suggests that the end groups (BH_3 and NMeH_2) are extremely labile and can be removed even under mild ionization conditions. However, the fact that the end groups were different in positive and negative mode suggested that they may be generated by the ionization process and are not necessarily the end groups present in the as-synthesized samples of polymer **8a**.

(iii) Matrix Assisted Laser Desorption/Ionization Time of Flight (MALDI-TOF). For higher molecular weight species, matrix assisted laser desorption/ionization time-of-flight (MALDI-TOF) is often the method of choice for analysis. We explored a variety of conditions, but for the only conditions under which we could observe polyaminoborane **8a** (2,5-dihydroxybenzoic acid, matrix/analyte ratio 1:2; reflective positive mode), the maximum laser strength was not sufficient to produce satisfactory signal-to-noise ratios for the polymers and the broad and ill-defined peak shape suggested the formation of metastable ions. This made MALDI-TOF a poor technique for the analysis of polymer **8a**. It was, however, possible to identify two series of peaks with an approximate spacing of 43 mass units, corresponding to the monomer repeat unit $[\text{MeNH-BH}_2]$ up to a degree of polymerization (DP_N) of approximately 33 (see Figure SI 19).

(b) Structural Characterization by Solid State NMR. **(i) Characterization of Poly(*N*-methylaminoborane), $[\text{MeNH-BH}_2]_n$ (**8a**), by Solid State NMR.** While poly(*N*-methylaminoborane) **8a** is soluble in various solvents and can be analyzed by standard solution NMR spectroscopy, we were not able to determine any end group functionality by ¹¹B or ¹H NMR. In solid state NMR spectroscopy on the other hand, the ability of macromolecules to undergo rotational and translational motion is greatly reduced, which makes it easier to detect the end groups. For this purpose, we performed a Multiple-Quantum Magic-Angle Spinning (MQMAS) experiment in order to analyze whether there were different boron environments and possible end groups present in **8a**. ¹¹B MQMAS NMR experiments are commonly used to differentiate between a true resonance and a second-order quadrupole line shape and to determine the isotropic chemical

(73) Pramanik, B. N.; Ganguly, A. K.; Gross, M. A. *Applied Electrospray Mass Spectrometry - Vol. 32 of the Practical Spectroscopy Series*; Marcel Dekker: New York, 2002.

(74) Wilm, M.; Mann, M. *Anal. Chem.* **1996**, *68*, 1.

(75) Schultz, G. A.; Corso, T. N.; Prosser, S. J.; Zhang, S. *Anal. Chem.* **2000**, *72*, 4058.

(76) Guaratini, T.; Gates, P. J.; Cardozo, K. H. M.; Campos, P. M. B. G. M.; Colepiccolo, P.; Lopes, N. P. *Eur. J. Mass Spectrom.* **2006**, *12*, 71.

(77) Guaratini, T.; Gates, P. J.; Pinto, E.; Colepiccolo, P.; Lopes, N. P. *Rapid Commun. Mass Spectrom.* **2007**, *21*, 3842.

(78) When the voltage was decreased to +75 V the distribution at lower molecular weight disappeared. See Figure SI 17. For the nanospray measurement at -125 V, see Figure SI 18.

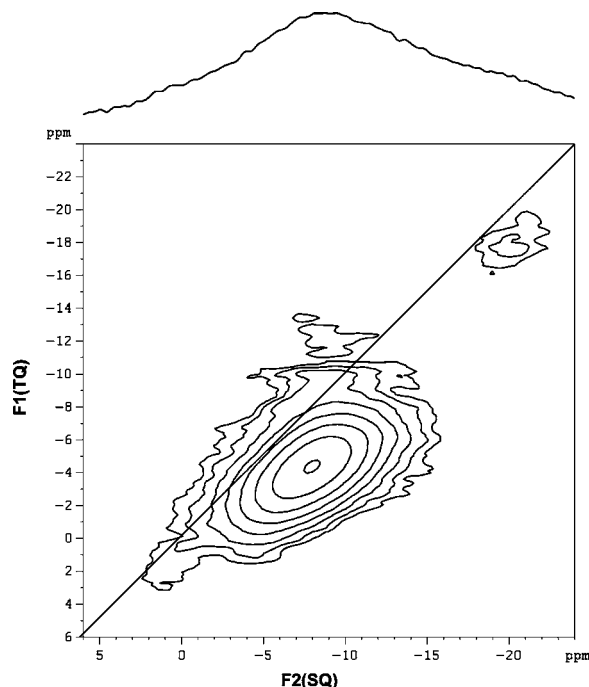


Figure 4. ^{11}B MAS NMR: sheared triple-quantum filtered MQMAS spectrum for poly(*N*-methylaminoborane) **8a**, prepared by using catalyst IrH_2POCOP **5**. $M_w = 214\,000$, PDI = 2.0 by GPC.

shift. By contrast, several maxima or shoulders can appear in a one-dimensional ^{11}B MAS NMR spectrum, which all belong to the same boron environment. The ^{11}B MQMAS NMR spectra of **8a** revealed that there were indeed different environments (Figure 4). Thus, we observed an intense signal ($\delta_{\text{iso}} = -5.8$ ppm, SOQE = 1.5 MHz, SOQE = second-order quadrupolar effect), which we assigned to the midchain $-\text{BH}_2-$ groups by comparison with the solution state NMR (^{11}B NMR (CDCl_3), $\delta = -6.7$ ppm)). We also found a very weak peak ($\delta_{\text{iso}} = -18.6$ ppm, SOQE = 1.2 MHz), which we attribute to end groups present in the sample as the chemical shift is similar to that for the BH_3 group in *N*-methylamine-borane adduct **7** (^{11}B NMR (CDCl_3), $\delta = -19.4$ ppm). As this peak is of too low intensity to reliably integrate relative to the resonance from the main chain, these data are consistent with the identity of the polymer **8a** as a linear material of substantial molecular weight.⁷⁹

(ii) Characterization of Polyaminoborane $[\text{NH}_2\text{BH}_2]_n$ (8d**) by Solid State NMR.** From the perspective of hydrogen storage, the insoluble parent polyaminoborane **8d** is of substantial interest as an intermediate in the dehydrogenation process for ammonia-borane **4**. As the material is insoluble, there is still some uncertainty whether the solid that can be isolated after catalytic dehydrocoupling of **4** with Brookhart's catalyst **5** is cyclic (e.g., a cyclic pentamer)³² or linear in nature. We were not able to observe cyclic oligomers such as $[\text{NH}_2-\text{BH}_2]_5$ by ESI-MS, nanospray, or MALDI-TOF and therefore further analyzed **8d** by ^{11}B MAS NMR spectroscopy. We prepared a sample of the unsubstituted insoluble polyaminoborane **8d** by the Ir-catalyzed dehydrogenation reaction of ammonia-borane (0.5 M, 0.1 mol % IrH_2POCOP , THF, 20 °C) and subsequent purification by washing the samples with THF in the glovebox.

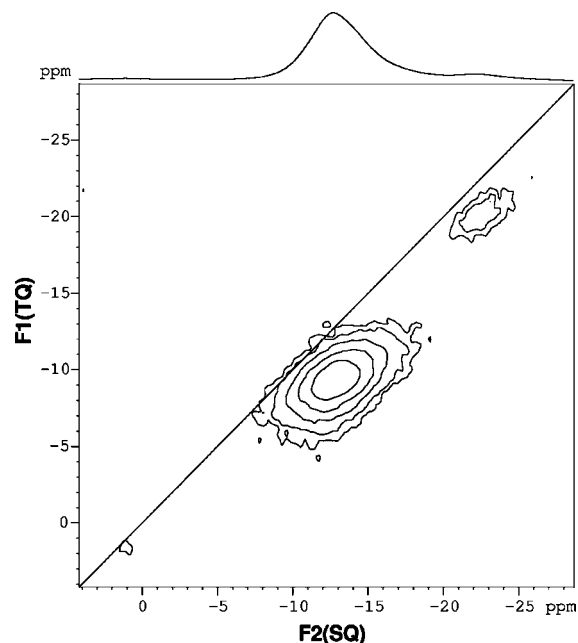


Figure 5. ^{11}B MAS NMR sheared triple quantum-filtered MQMAS spectrum of the unsubstituted polyaminoborane **8d**.

As for the case of **8a**, the ^{11}B MQMAS NMR spectra for polyaminoborane **8d** showed a low intensity end group signal assigned to BH_3 groups ($\delta_{\text{iso}} = -21.0$ ppm, SOQE = 1.4 MHz) in addition to the much more intense signal for the main chain boron atoms ($-\text{BH}_2-$) ($\delta_{\text{iso}} = -10.7$ ppm, SOQE = 1.5 MHz) (Figure 5).

These peak assignments seem reasonable if the spectrum is compared to the solution ^{11}B NMR spectrum of ammonia-borane (**4**) (^{11}B NMR (THF), $\delta = -23$ ppm) and that of 1:1 copolymer **8c**, which displayed a broad peak at -11 ppm. In addition, the solution ^{11}B NMR signal for the cyclic borazane analog $[\text{NH}_2-\text{BH}_2]_3$ is reported to be -11.4 ppm (in MeCN),⁸⁰ a similar value to that assigned to the main chain boron atoms ($-\text{BH}_2-$) of **8d**. The ^{11}B MAS NMR spectrum of the starting material **4** was straightforward to distinguish from that of polymer **8d** because of its sharper line shape ($\delta_{\text{iso}} = -23.3$ ppm, SOQE = 1.46 MHz). Thus the ^{11}B MAS NMR spectra confirmed that the purified polymer did not trap any ammonia-borane starting material (**4**). Second-order quadrupolar effect parameters up to 2 MHz are typical of tetrahedrally coordinated boron. In contrast to the situation for **8a**, the peak intensity for the end group of **8d** was sufficient to allow an approximate comparative integration versus the main chain signal. The relative peak intensities indicate that the end group boron atom to chain boron atom ratio is around 1:20 corresponding to an approximate degree of polymerization of around 20. Unfortunately, line shape analysis of broad unresolved peaks is associated with relatively large uncertainties.⁸¹

The solid state ^{11}B MAS NMR spectrum of **8d** differed substantially from those reported for the materials described earlier using different syntheses of what might have been expected to be the unsubstituted polyaminoborane $[\text{NH}_2-\text{BH}_2]_n$.^{13c,d,82} For example the material prepared by Kim

(79) The solution ^{11}B NMR spectrum for this sample did not show any detectable shoulder in this region. We therefore conclude that the peak in the solid state NMR does not arise from a residual monomer.

(80) Wang, J. S.; Geanangel, R. A. *Inorg. Chim. Acta* **1988**, *148*, 185.

(81) Avadhut, Y. S.; Schneider, D.; Schmedt auf der Gönne, J. *J. Magn. Reson.* **2009**, *201*, 1.

(82) Gervais, C.; Babonnaeu, F. *J. Organomet. Chem.* **2002**, *657*, 75.

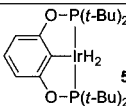
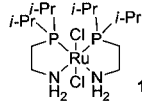
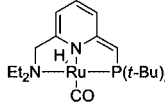
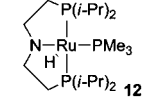
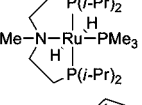
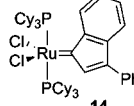
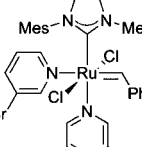
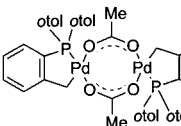
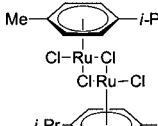
from the thermolysis of NaBH_4 and $(\text{NH}_4)_2\text{SO}_4$ showed three peaks: a very broad resonance from ca. 15 to 25 ppm assigned to three-coordinate boron in B_3N_3 ring environments and a more intense broad peak together with a small broad resonance at ca. -25 and -35 ppm, respectively, assigned to four-coordinate boron.^{13c} It should be noted that, although δ_{iso} was not reported for any of the various materials and the line shape at different magnetic fields may distort the observed value, the detection of several peaks in the regions characteristic of three- and four-coordinate boron indicates that the structure of these materials is substantially more complex, with a larger number of different boron environments, compared to the essentially linear material obtained in this work. Thus polyaminoborane **8d** obtained from the catalytic dehydrogenation of **4** by Ir catalyst **5** contained only tetracoordinate $-\text{BH}_2-$ main chain environments and low intensity $-\text{BH}_3$ end groups.

Polymer **8d** was also analyzed by ^1H MAS NMR. However, the spectrum suffered from strong $^1\text{H}-^1\text{H}$ and $^1\text{H}-^{11}\text{B}$ dipolar couplings. Small amounts of trapped solvent were detected as these gave rise to sharp peaks because of rapid molecular tumbling. Polymer **8d** gave rise only to a single broad peak with an isotropic chemical shift range of 1–6 ppm. In comparison for the starting material **4**, ^1H MAS NMR showed two peaks at 0.8 and 4.1 ppm for the BH and NH environments, respectively.

(4) Investigation of Other Catalysts for the Polymerization of $\text{MeNH}_2\cdot\text{BH}_3$ (7). Brookhart's Ir-pincer complex (**5**) is not commercially available and has to be prepared in three steps.⁵⁴ In addition, we have found that this complex is very substrate specific and only catalyzes the dehydropolymerization of a limited range of amine-borane adducts with sterically unencumbered *n*-alkyl substituents at nitrogen.^{55,83} An exploration of other catalysts is therefore important as more readily available examples that permit the dehydropolymerization of a broader range of amine-borane adducts may be discovered. Here we report studies of a range of other potential catalysts for the dehydrogenative polymerization of **7**. Of particular interest was an exploration of the features of the catalyst which made it suitable for the formation of linear polymers instead of small cycles or borazine, a product from the formal release of a second equivalent of dihydrogen from the amine-borane adduct precursor. To this end, we screened a variety of catalysts under standardized conditions; 0.3 mol % catalyst in THF (10 M) at 20 °C for 20 h (see Table 2).

We found that a variety of pincer catalysts were highly active and produced high molecular weight polyaminoborane **8a** cleanly and in good yields. These included Milstein's catalyst (**11**)⁸⁴ (Table 2, entry 3) and related ruthenium complexes **12** and **13** first described by Schneider and co-workers (Table 2, entries 4²⁹ and 5⁸⁵). These reactions proceeded rapidly, but in the case of **11**, there appeared to be an induction period of several minutes before the onset of visible hydrogen evolution, most likely due to the dissociation of the CO ligand and formation of a vacant coordination site. Morris's catalyst (**10**),⁸⁶ first used by Fagnou²⁷ to release dihydrogen from amineboranes, also gave polymer **8a** at -20 °C, but at room temperature the reaction was irreproducible (Table 2, first entry

Table 2. Different Catalysts for the Dehydropolymerization of $\text{MeNH}_2\cdot\text{BH}_3$ (**7**)

Entry	Catalyst	Isolated Yield / %	M_w	PDI
1		60 ^{a)}	160 000	2.9
2	 + 30 equiv. KOtBu with respect to cat.	59 ^{b)} 92 ^{c)}	23 000 89 000	2.5 3.4
3		61 ^{d)} 81 ^{e)}	92 000 92 000	3.2 1.2
4		90	460 000	2.6
5		71	344 000	1.8
6		41	20 000	7.8
7		72	10 000	3.0
8		47 ^{f)}	16 000	7.6
9	Rh on alumina 17	40 ^{g)}	26 000	8.5
10	$\text{Rh}_2(\text{OC}(\text{O})\text{CF}_3)_4$ 18	42	60 000	3.1
11	$\text{Rh}_2(\text{OAc})_4$ 19	71	31 000	6.9
12	$[\text{Rh}(\text{piv})_2]_4$ ^{h)} 20	86 ⁱ⁾	31 000	8.1
13		58	8 000	13
14	$[\text{Rh}(\mu\text{-Cl})(1,5\text{-cod})]_2$ 2	75	42 000	10.5
15	$(\text{Ph}_3\text{P})_3\text{RuCl}_2$ 22	76	7 800	6.3

^{a)} 2 min 0 °C, then 20 min 20 °C. ^{b)} 88% purity based on ^{11}B NMR spectroscopy; remainder: unidentified side products. ^{c)} 15 min at -20 °C and then 30 min at -10 °C, 0.3 mol % catalyst. ^{d)} 97% purity based on ^{11}B NMR spectroscopy; remainder: starting material. ^{e)} 2 h 40 min. ^{f)} 70% pure; remainder: unidentified side products. ^{g)} In 64% purity based on ^{11}B NMR spectroscopy; remainder: starting material. ^{h)} piv = pivalate ($[(t\text{-BuCO}_2)]^-$). ⁱ⁾ In 92% purity based on ^{11}B NMR spectroscopy; remainder: starting material.

(83) Staubitz, A.; Manners, I. Unpublished results.

(84) Zhang, J.; Leitus, G.; Ben-David, Y.; Milstein, D. *J. Am. Chem. Soc.* **2005**, *127*, 10840.

(85) Friedrich, A.; Drees, M.; Schmedt auf der Günne, J.; Schneider, S. *J. Am. Chem. Soc.* **2009**, *131*, 17552.

2).⁸⁷ On addition of the catalyst to the reaction mixture at 20 °C a strong exotherm was detected with vigorous bubbling of the yellow solution. In most attempts the reaction initially became viscous, but rarely to the same degree as with other catalysts that gave polymer **8a**, and precipitation often only gave a very low isolated yield. When a sample of preformed polymer **8a** was treated with **10** (THF, 0.2 mol %, 20 °C), initial bubbling was observed, and by ¹¹B NMR spectroscopy we observed the formation of a broad doublet at 33.1 ppm ($J_{BH} = 120.0$ Hz) (Figure SI 20).⁸⁸ It was therefore reasonable to assume that catalyst **10** was too reactive under the conditions used. In order to obtain more reliable results, the reaction was performed at lower temperature (−20 °C for 15 min, then at −10 °C for 30 min) with only half the catalyst loading (0.15 mol %). Under these conditions, hydrogen evolution was less rapid and reproducible results could be obtained (Table 2, second entry 2).

Significantly, the pincer motif was found not to be a prerequisite for an active catalyst. Carbene-based reagents, such as Neolyst (**14**) and Grubbs' third generation catalyst (**15**), also yielded polymer **8a**, although the conversion in 20 h at room temperature and molecular weight were relatively low (Table 2, entries 6 and 7 respectively). When the reaction was allowed to proceed for 2.5 days, slightly more monomer was converted, but we also observed additional product peaks (¹¹B NMR: $\delta = 5.5$ ppm and 4.9 ppm).

The use of a carbene motif as a ligand in the catalyst for amine-borane dehydrocoupling was first introduced by Baker and co-workers using Ni(NHC)₂ catalysts (NHC = *N*-heterocyclic carbenes), which was able to release almost 3 equiv of hydrogen from ammonia-borane in diglyme at 60 °C.³⁷ The mechanism for this reaction has sparked an interesting debate, but there is a general agreement that there is some participation of the ligand, which is protonated by the amine-borane during the reaction.^{89–91} It is conceivable that the future use of chiral NHC ligands may lead to some tacticity control in the synthesis of **8a** and related materials.

We also screened a range of Rh(II) and Rh(I) complexes, the latter of which have previously been reported to give borazines at slightly elevated temperatures. All of the species tested appeared to be rapidly reduced to Rh(0) (as determined by a color change to black), and all gave moderate to low molecular weight polymer **8a**, relatively slowly. Significantly [Rh(μ -Cl)(1,5-cod)]₂, which has previously been reported to give borazine [MeN–BH]₃ at 45 °C in DME,²⁴ was found to catalyze the dehydropolymerization of **7** to give moderate molecular weight **8a** with an extremely high PDI (10.5) (Table 2, entry 14).⁹² It is likely that the polyaminoboranes are the preferred kinetic products instead of small oligomeric cycles as otherwise

we would not expect to observe any polymer formation at all. However, it appears that borazines are thermodynamically favored over the polyaminoboranes **8a** (cyclic or linear), partly due to the entropic gain associated with hydrogen gas release and formation of small molecules from polymeric precursors. Borazines are also more stable than the prospective polyiminoboranes which would be obtained by a further dehydrogenation step, which has also been predicted by computational studies.⁹³

Herrmann's catalyst (**16**) (Table 2, entry 8) also gave polymer, but the reaction was sluggish and side reactions were detected, which was perhaps not surprising given that so far palladium based catalysts have been shown to be comparatively ineffective for dehydrocoupling reactions.²⁴ The attempted polymerization of **7** with Jacobsen's salen catalyst ((*R,R*)-*N,N'*-bis(3,5-di-*tert*-butylsalicylidene)-1,2-cyclohexanediamino manganese(III) chloride),⁹⁴ gave no conversion, even when sodium tetrakis[(3,5-trifluoromethyl)phenyl]borate (Na[B(3,5-(CF₃)₂C₆H₃)₄]) was added to sequester the chloride ligand. Likewise, despite the fact that Crabtree's catalyst ([IrPCy₃pyr(1,5-cod)]PF₆) is a very efficient hydrogenation catalyst, no conversion of **7** to **8a** was observed.⁹⁵

The microstructure of the polyaminoborane **8a** formed using the various catalysts is interesting to compare with the analogous material formed using Ir catalyst **5**. Indeed, when other catalysts such as the Ru carbene complex **14** were used we observed an additional distribution in the positive ionization mode by ESI-MS analysis of **8a**, which appears to correspond to a radical ionization of the cyclic polymer [(MeNH–BH₂)_n–H]⁺ (see peak at *m/z* 1412.96 in Figure SI 21). This distribution was not detected in the case of the polymeric material **8a** (see Figure 2) formed from the Ir(III)-complex **5**. We tentatively postulate that this might be evidence for the formation of a cyclic polyaminoborane component in addition to linear species.

Another interesting feature involved the peak shapes of the *N*-methyl groups in the polymer backbone of poly(*N*-methylaminoborane) **8a**, by ¹³C and in particular ¹H NMR spectroscopy (Figures SI 22 and SI 23). While all catalysts gave polymers where these peaks were broad with shoulders, an overlay of these spectra showed that the actual peak shape varied significantly when different catalysts were used, but the spectra were reproducible when different samples were prepared under the same conditions using the same catalyst. These differences became even more obvious when the peak shapes obtained in a H–C correlation experiment (gradient band selective heteronuclear single quantum coherence spectrum, gbsHSQC) were used (Figures SI 24 to SI 27). These results may indicate that the catalyst is capable of influencing the tacticity of polyaminoborane **8a**, which should inspire significant future research.⁹⁶

Discussion

In the first experiments described in our brief initial report,⁵⁵ all polymerizations using the Ir catalyst **5** to give poly(*N*-methylaminoborane) **8a** from **7**, the related copolymers such as **8b** and **8c** derived from **7** and **4**, and poly(*N*-*n*-butylami-

(86) Clapham, S. E.; Hadzovic, A.; Morris, R. H. *Coord. Chem. Rev.* **2004**, *248*, 2201.

(87) Fagnou and co-workers briefly noted the formation of poly(*N*-methylaminoborane) using their Ru catalyst system based on ¹¹B NMR evidence.²⁷

(88) While the chemical shift is very similar to that of borazine [31.7 ppm ($J_{BH} = 130$ Hz): Beachley, O. T., Jr. *Inorg. Chem.* **1969**, *8*, 981; 32.5 ppm ($J_{BH} = 134$ Hz): Nöth, H. *Angew. Chem.* **1961**, *73*, 371], based on the different coupling constant ($J_{BH} = 120$ Hz) we believe that the peak may arise from *N*-methyliminoborane environments –MeN=BH– in the polymer chain.

(89) Zimmerman, P. M.; Paul, A.; Zhang, Z. Y.; Musgrave, C. B. *Angew. Chem., Int. Ed.* **2009**, *48*, 2201.

(90) Yang, X.; Hall, M. B. *J. Organomet. Chem.* **2009**, *694*, 2831.

(91) Yang, X. Z.; Hall, M. B. *J. Am. Chem. Soc.* **2008**, *130*, 1798.

(92) A full investigation of this reaction will be the subject of a future publication.

(93) Abdurahman, A.; Albrecht, M.; Shukla, A.; Dolg, M. *J. Chem. Phys.* **1999**, *110*, 8819.

(94) Larrow, J. F.; Jacobsen, E. N. *Org. Synth.* **2004**, *10*, 96.

(95) However, a stoichiometric reaction did take place which led to two new products with singlet resonances by ¹¹B{¹H} NMR that split into triplets in the ¹H coupled spectrum (in THF-*d*₈): Peak 1, 73%, $\delta = -3.7$ ppm, $J = 115.5$ Hz; Peak 2, 27%, $\delta = -8.9$ ppm, $J = 116.7$ Hz.

noborane) from $n\text{-BuNH}_2\cdot\text{BH}_3$ were performed at high concentrations of substrate (10 M or without solvent). This was based on our experience with the synthesis of the related polyphosphinoboranes,^{49–52} where solvent-free conditions were required to obtain high molecular weights. The apparent requirement of high substrate concentrations for polymer formation was further reinforced by a report by Goldberg and Heinekey that described how low concentrations (ca. 0.5 M in substrate **7**) with the same Ir catalyst (**5**) at a loading of 1 mol % led to the formation of oligomers as determined ESI-MS with a mass range up to 2200 m/z and a maximum for the distribution at ca. 850 m/z corresponding to ca. 20 repeat units.⁵⁸ However, our further studies of the influence of the substrate concentration at constant catalyst loading on the molecular weight described in this manuscript showed that materials with a high molecular weight are also formed from similarly dilute reactions with even lower catalyst loadings (0.1 mol %) (section 2 (b), Table SI 4, entries 1 and 14). Moreover, we found ESI mass spectrometry to give voltage dependent spectra that considerably underestimate the true molecular weight revealed by GPC and DLS measurements. Nevertheless, we have also shown that lower molecular weight **8a** was indeed formed at low substrate conversion (<40%, Section 2 (c)) and the samples analyzed in the ESI mass spectrometry experiments by Goldberg and Heinekey may indeed have an oligomeric structure if they originated under such conditions.

The nature of the polyaminoborane **8d** formed by the dehydrogenation of ammonia-borane $\text{NH}_3\cdot\text{BH}_3$ catalyzed by Ir catalyst **5** is of considerable interest from the perspective of hydrogen storage. Thus, the ability to chemically regenerate **4** from **8d** will depend to a significant degree on its chemical structure. Analysis of **8d** by solid state NMR was consistent with an essentially linear main chain of alternating four-coordinate boron and nitrogen atoms as only one major peak was present with an appropriate chemical shift and we could determine the presence of end groups. Even though the broadness of the peaks made an exact quantification impossible, we were able to estimate an approximate chain length of around 20 repeat units (if we assume that there are no cyclic species present as well). In this context it is important to note that the observed chemical shifts for **8d** ($\delta_{\text{iso}} = -10.7$ ppm for $-\text{BH}_2-$ in the chain and $\delta_{\text{iso}} = -21.0$ ppm for the $-\text{BH}_3$ end group) are in very good agreement with those calculated for a linear pentamer ($\delta_{\text{iso}} = -9.5$ to -11.8 ppm for $-\text{BH}_2-$ in the chain and $\delta_{\text{iso}} = -23.0$ ppm for the end group $-\text{BH}_3$, DFT/GIAO calculation) but correspond less well to a branched structure ($\delta_{\text{iso}} = -5.9$ ppm for a branching group $-\text{BH}$, DFT/GIAO calculation).⁹⁷ More recently, the BN-analog of butane, $\text{NH}_3-\text{BH}_2-\text{NH}_2-\text{BH}_3$, has also been synthesized. This compound showed chemical shifts (in THF- d_6) of $\delta = -11.6$ ppm

for the $-\text{BH}_2-$ group and -22.8 ppm for the BH_3 group, which lends further support to our assignment of **8d** as a linear polymer.⁹⁸

A comparison of the WAXS data of our material with those described for the cyclic pentamer **6**, reported by Shore and co-workers,⁹⁹ also indicated that the materials were different.¹⁰⁰ Furthermore, while the IR spectra of **8d** and Shore's species **6** are very similar for the N–H and B–H stretching modes (only small differences of about 3 cm^{-1} for the corresponding bands), the fingerprint region for the N–H deformation modes varied substantially. Polymer **8d** possessed a sharp band at 1557 cm^{-1} , whereas **6** showed a band at 1571 cm^{-1} . Additionally, cyclic pentamer **6** was reported⁹⁹ to be soluble in DMSO, whereas we were not able to dissolve **8d** in any common organic solvent.

Analysis of the IR spectra also showed that **8d** was not the same material as any of the polyaminoboranes prepared by other routes and reported in the literature.^{13a,c,d} For example, in the N–H stretching region, **8d** showed sharp bands, whereas for the other materials the bands were broad. These materials also similarly differed in the B–H and fingerprint region, albeit to a lesser extent. Most convincingly, solid state NMR measurements for **8d** showed that it has a much simpler structure than the other materials. Thus, the ^{11}B MAS NMR for **8d** showed a major peak and another assigned to end groups, whereas the materials prepared earlier by others showed numerous peaks, suggesting a variety of different three- and four-coordinate boron environments. The polyaminoborane materials obtained by other routes appear to possess a significant number of cyclic B_3N_3 units and may also be either branched or cross-linked rather than having an essentially linear polyaminoborane structure like **8d**. This hypothesis is further supported by the TGA results. The presence of rings, branching, and cross-linking generally leads to increased thermal stability for a material and a higher ceramic yield as loss of small molecular fragments is hindered. The ceramic yield of **8d** was 40% at $600\text{ }^\circ\text{C}$ by TGA, whereas the previously reported polyaminoboranes have ceramic yields of >70% even at more elevated temperatures. Taking all of the evidence together, we therefore conclude that the material **8d** formed using the Ir catalyst **5** in our hands is indeed an essentially linear polymer. The apparent low molecular weight of **8d** corresponding to ca. 20 repeat units is likely a result of premature precipitation of the insoluble material from THF during its formation. It should be also noted that such a conclusion is not unexpected based on the ESI mass spectrometry analysis of random copolymers **8b** and **8c**, which suggests that **4** is equally capable as **7** of forming linear polymer chains. The WAXS pattern that we observed for a sample of **8a** prepared using catalyst **5** suggests an amorphous polymer had formed, whereas polymer **8d** gave one main peak, suggesting a semi-crystalline material. This is in contrast to the work by Goldberg and Heinekey, where a WAXS pattern assigned to the cyclic pentamer $[\text{NH}_2-\text{BH}_2]_5$ was detected.^{32,101}

Although we can only speculate about the details of the mechanism of the polymerization of **7** by the Ir catalyst **5**, our results described in this paper provide some useful insight into

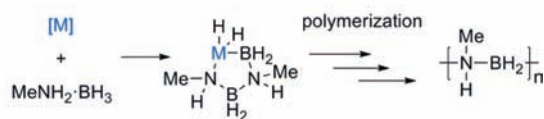
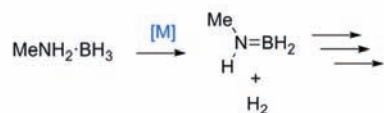
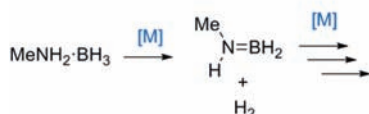
(96) Polymer **8d** could also be obtained using a Ru(II) catalyst **12**, first described by Schneider and co-workers.²⁹ As for the case of **8a**, the ^{11}B MQMAS NMR spectra for polyaminoborane **8d** showed a low intensity end group signal ($\delta_{\text{iso}} = -21.0$ ppm, SOQE = 1.4 MHz) in addition to the much more intense ^{11}B NMR signal for the main chain boron atoms ($-\text{BH}_2-$) ($\delta_{\text{iso}} = -10.7$ ppm, SOQE = 1.5 MHz). However, the ratio of the relative intensities suggested that the sample contained a higher concentration of end groups and was therefore of lower molecular weight than that prepared using **5**.

(97) Bluhm, M. E.; Bradley, M. G.; Butterick, R., III; Kusari, U.; Sneddon, L. G. *J. Am. Chem. Soc.* **2006**, *128*, 7748.

(98) Chen, X.; Zhao, J.-C.; Shore, S. G. *J. Am. Chem. Soc.* **2010**, *132*, 10658.

(99) Bøddeker, K. W.; Shore, S. G.; Bunting, R. K. *J. Am. Chem. Soc.* **1966**, *88*, 4396.

(100) Shore reported for the cyclic pentamer, $[\text{NH}_2-\text{BH}_2]_5$ (**6**), d -spacings of 4.38 (m), 3.80 (vs), 2.87 (w), 2.19 (m), 2.11 (vw), 1.90 (w), 1.67 (vw), 1.54 (vw), 1.42 (vw), 1.26 (vw) Å (with vs = very strong, m = medium, w = weak, vw = very weak). NMR data were not recorded at the time.⁹⁹

Scheme 1. Possible Mechanisms for the Catalytic Dehydropolymerization Route to Poly(*N*-methylaminoborane) **8a****(a) Polymer chain growth at the metal center****(b) Polymer chain growth removed from the metal center****(c) Dual action of the metal center**

the general features of the process. Some of the likely mechanistic scenarios are outlined in Scheme 1. The first involves the growth of the polymer chain from the metal center, with the amine-borane adduct as the true monomer, a process initially proposed by Baker and Dixon for the catalytic dehydrogenation of ammonia-borane with **5** (Scheme 1a).¹⁰² A second possibility is that the catalyst merely dehydrogenates the amine-borane adduct, leading to hydrogen evolution and the free aminoborane, MeNH=BH₂, which could then polymerize by itself, by either addition polymerization or an autocatalytic process with the residual amine-borane adduct or an existing polymer chain (Scheme 1b). This mechanism is analogous to that described by Paul, Musgrave and co-workers for the reaction of **4** with Ir-complex **5** as a catalyst.¹⁰³ A third mechanism can also be considered where the metal first dehydrogenates the amine-borane adduct and then, in a second step, also subsequently catalyzes the subsequent polymerization of the resulting aminoborane monomer in a manner analogous to the case of a Ziegler–Natta catalyst in olefin polymerization (Scheme 1c).

The essential chain-growth nature of the reaction revealed by molecular weight versus conversion studies was unexpected, because the dependence of the molecular weight on the catalyst loading (higher loadings afforded higher molecular weight polymers) suggested a step-growth process. For a chain-growth polymerization an increase in the number of initiating sites would lead to shorter polymer chains and thus a higher catalyst loading should give a lower molecular weight for the resulting polyaminoborane. This suggests that the first mechanism (Scheme 1a) is not correct, at least in its unmodified form. It is also possible to exclude the second mechanism (Scheme 1b), where the function of the metal is merely to produce the aminoborane monomer. If this were the case, then the microstructures of the resulting samples of polymer **8a** would be

expected to be identical under the same reaction conditions, even with different catalysts. Based on the significant variation in the ¹H NMR peak shapes for the methyl group in **8a**, we concluded that the relative ratios of the diastereomeric environments for the methyl peak (i.e., the tacticity) varied with different catalysts (see Figures SI 24–27). This situation is most likely to arise if the relative energies for the transition states for the polymer growth reaction are different, which would not be the case if the actual polymerization step was the same, irrespective of the catalyst. Furthermore, ESI-MS spectra observed under the same conditions for **8a**, prepared with different catalysts showed different distributions of products (compare, for example, Figure 2 for catalyst **5** and Figure SI 21 for catalyst **14**, where evidence for cyclic polyaminoborane **8a** at *m/z* = 1412.96 is present in the latter case). Another possibility which cannot be completely discounted at this stage is that the polymers may have a slightly different primary structure with the degree of branching dependent on the catalyst. However, by ¹¹B NMR there were no signals suggesting a significant number of boron environments other than the main chain –BH₂– groups for the linear polymer obtained using catalysts other than IrH₂POCOP **5**.

The third mechanism, on the other hand, appears to account for the experimental observations to date in the most satisfactory manner. The observed molecular weight versus conversion plot (Figure 1) is consistent with a fast chain-growth polymerization process that is preceded by a slower step involving the generation of an aminoborane monomer from the amine-borane adduct precursor. For such a sequential reaction, the formation of a high molecular weight polymer would be expected to depend on the availability of the true monomer (the aminoborane, MeNH₂·BH₃ **7**), thereby accounting for the observation that at low conversions (<40%) the molecular weight grew with increasing conversion (Figure 1) and that higher catalyst loadings led to higher molecular weights. The polymerization of the aminoborane monomer at the metal center in the second step would also explain the evidence for catalyst-dependent tacticity of the polymer, as steric and electronic effects associated with the metal and ancillary ligation would be expected to influence the stereochemistry of the process. Furthermore, this proposal is qualitatively supported by mechanistic studies of the dehydrocoupling of the secondary amine-borane adduct Me₂NH·BH₃ by Ru catalyst **12**²⁸ and in situ generated Cp₂Ti as catalyst.¹⁰⁴ Both the aminoborane, Me₂N=BH₂, and linear diborazane, Me₂NH–BH₂–NMe₂–BH₃, were identified as intermediates. Reaction kinetics and thermodynamic calculations suggest both adduct dehydrogenation and diborazane formation to be metal catalyzed reactions. This is further supported by the study of amine-borane oligomers complexed to Rh centers where potential intermediates in the catalytic dehydrocoupling process were successfully isolated.¹⁰⁵ In addition, there are several recent studies showing that aminoboranes can bind to transition metal centers and which indicate that the metal can be directly involved in further transformations of these species.^{106–108} Similar intermediates have also been postulated and/or isolated for main group metal complexes.¹⁰⁹ Further investigations into

(101) It is also in contrast to our own earlier report, where we observed a *d*-spacing of 3.6 Å,⁵⁵ but we now believe that a contribution from residual trapped ammonia-borane **4** is likely, and this species can only be removed by extensive washing of the sample with THF, as was the case in this paper.

(102) Pons, V.; Baker, R. T.; Szymczak, N. K.; Heldebrant, D. J.; Linehan, J. C.; Matus, M. H.; Grant, D. J.; Dixon, D. A. *Chem. Commun.* **2008**, 6597.

(103) Zimmerman, P. M.; Paul, A.; Zhang, Z.; Musgrave, C. B. *Inorg. Chem.* **2009**, *48*, 1069.

(104) Sloan, M. E.; Staubitz, A.; Clark, T. J.; Russell, C. A.; Lloyd-Jones, G. C.; Manners, I. *J. Am. Chem. Soc.* **2010**, *132*, 3831.

(105) Douglas, T. M.; Chaplin, A. B.; Weller, A. S.; Yang, X.; Hall, M. B. *J. Am. Chem. Soc.* **2009**, *131*, 15440.

(106) Dallanegra, R.; Chaplin, A. B.; Tsim, J.; Weller, A. S. *Chem. Commun.* **2010**, *46*, 3092.

(107) Alcaraz, G.; Vendier, L.; Clot, E.; Sabo-Etienne, S. *Angew. Chem., Int. Ed.* **2010**, *49*, 918.

the mechanism of this polymerization may be fruitful because if the polymer grows from the catalytic center, considerable tacticity control may be achievable using chiral ligands.

Summary

The dehydropolymerization of *N*-methylaminoborane **7** using Brookhart's Ir pincer catalyst (**5**) to give high molecular weight poly(*N*-methylaminoborane) **8a** has been achieved. The analogous reaction with ammonia-borane (**4**) afforded an insoluble material (**8d**); however, the formation of soluble random copolymers (**8b** and **8c**) was possible from mixtures of **4** and **7**. Evidence for the polymeric rather than oligomeric nature of **8a–8c** was provided by GPC and DLS studies. Detailed structural analysis of **8a** using various mass spectrometric techniques, such as high resolution ESI and nanospray MS, solution and solid state NMR, and IR spectroscopy, gave important insight into the molecular structure of these polymers and was consistent with an essentially linear polymeric structure. Evidence was also provided that insoluble polymer **8d** is also an essentially linear material with around 20 repeat units based on end group analysis of ^{11}B MAS NMR spectra. The lower molecular weight of **8d** is presumably due to premature precipitation from the reaction solution during its formation.

The formation of **8a** from **7** using the Ir catalyst **5** was studied in detail. Significantly, variation of the catalyst loading highlighted a dependence of the polymer molecular weight on this parameter, where higher loadings led to a higher molecular weight polymer (**8a**). In addition, molecular weight versus conversion studies were consistent with a chain-growth rather than a step-growth mechanism but with a region where polymer chain length was small and conversion-dependent at low substrate conversion (<40%). The results obtained are consistent with a two-stage polymerization mechanism where, first, the Ir catalyst **5** dehydrogenates **7** to afford the monomer $\text{MeNH}=\text{BH}_2$ and, second, the same catalyst effects the subsequent polymerization of this species.

A variety of Ru, Rh, and Pd catalysts were also found to be active for the dehydropolymerization of **7** to afford polyaminoborane **8a**. The catalyst screening revealed that the pincer motif was not a necessary requirement for dehydropolymerization; however catalysts possessing this type of ligand were found to be the most active. Significantly, evidence was obtained for catalyst-dependent tacticity.

The finding that a variety of Ru, Rh, and Pd catalysts are active for the polymerization is potentially significant as one of the major limitations of the Ir catalyst **5** is the restricted range of amine-borane adducts $\text{RNH}_2\cdot\text{BH}_3$ ($\text{R} = \text{H}$ and *n*-alkyl groups) that can successfully be polymerized. Even groups such as benzyl substituents lead to amine-borane substrates that resist polymerization using **5**.⁸³ If polyaminoboranes are to find a wider range of applications, it will be necessary to be able to access a variety of structures. Future work will explore the use of the new catalyst systems to access a diverse range of polyaminoboranes, the introduction of chiral ligation at the metal centers to control polymer

tacticity, and detailed studies of the properties of the resulting materials as a prelude to the development of realistic applications.

Experimental Section

(1) General Procedures and Equipment. Reactions were performed under nitrogen or argon using dry solvents. IR spectra were measured using a Perkin-Elmer FT-IR spectrometer. NMR experiments were performed on JEOL ecp300 (300 MHz) and ecp400 (400 MHz) spectrometers in dry solvents. ESI mass spectra were recorded on a Bruker Daltonics Apex IV Fourier transform Ion Cyclotron resonance mass spectrometer, nanospray MS on a Applied Biosystems QStar-XL mass spectrometry using a Advion Biosciences nanomate chip-based nanospray source, and MALDI MS on a Applied Biosystems 4700 instrument. The solvent mixture used for injection was 1:4 THF/MeCN. GPC chromatograms were recorded on a Viscotek VE2001, using a flow rate of 1 mL/min in THF with 0.1 w/w % *n*-Bu₄NBr, calibrated for polystyrene standards, with an approximate injection concentration of 2 mg/mL unless otherwise stated. The columns used were of grade GP5000H_{HR} followed by GP2500H_{HR} (Viscotek) at a constant temperature of 30 °C. Dynamic light scattering experiments were performed using a Malvern Zetasizer Nano S spectrometer at $\lambda = 632$ nm in a glass cuvette using dry THF, dry THF with 0.1 w/w% of *n*-Bu₄NBr, or DMSO (dried over molecular sieves, 4 Å) at 25 °C, citing the average values for volume and intensity. The refractive indices (RI) for polymers **8a–8c** are unknown at present, and the measurements were run with an assumption of RI = 1.43 (slightly but not much higher than that for THF (RI = 1.409, Malvern instrument settings), as the sample gave a relatively weak positive Δ RI signal in GPC measurements in THF, and considerably lower than polystyrene (RI = ca. 1.6),¹¹⁰ which when run in THF gave a quite intense Δ RI signal in GPC measurements). TGA was run on a TGA Q500 apparatus at 10 °C/min. Solid-state NMR experiments were performed on a Bruker Avance DSX500 or a Bruker Avance III at a magnetic field of 11.74 T with a commercial 2.5 mm MAS double-resonance probe. The samples were spun at 20 kHz. The 1D spectra were corrected for background signals by subtraction. The chemical shift scale refers to 1% tetramethylsilane in CDCl₃ and BF₃·Et₂O in CDCl₃ for ^1H and ^{11}B at 0 ppm, respectively. The ^{11}B MQMAS was obtained using a triple-quantum filtered three-pulse sequence with a z-filter and ^1H continuous-wave decoupling.¹¹¹ The second-order quadrupolar effect (SOQE) parameters and the isotropic chemical shift values δ_{iso} were determined by moment analysis^{111,112} or fitting from projections taken from the sheared ^{11}B MQMAS spectra. X-ray powder diffraction data were collected with Cu K α radiation ($\lambda = 1.5418$ Å) on a Bruker D8 Advance powder diffractometer fitted with a 0.6 mm fixed divergence slit, knife-edge collimator, and a LynxEye area detector. Data were collected between 5° and 50° 2θ in $\theta/2\theta$ mode with a step width of 0.05°.

(2) Reagents. All reagents were obtained from commercial sources or prepared using reported procedures and used without further purification unless stated otherwise. Ammonia-borane was obtained from Aldrich and purified by sublimation ($T = 40$ °C, $p = 10^{-3}$ mbar) prior to use. THF and dioxane were distilled from Na; DMSO used for reactions was distilled twice from CaH₂. Ether and hexanes were dried using a Grubbs' solvent purification system.

(3) Molecular Weight versus Adduct Conversion Experiments. In the glovebox, in a custom-made Λ -shaped flask, the monomer solution of adduct **7** (112 mg, 2.50 mmol, in THF 4.75 mL) was placed in one-half and the catalyst **5** solution (0.25 mL from a stock solution, 18 mg in 3 mL THF; 0.0025 mmol, equals 0.1 mol % catalyst loading) in the other. This apparatus was then

- (108) (a) Tang, C. Y.; Thompson, A. L.; Aldridge, S. *J. Am. Chem. Soc.* **2010**, *132*, 10578. (b) Tang, C. Y.; Thompson, A. L.; Aldridge, S. *Angew. Chemie, Int. Ed.* **2010**, *49*, 921.
(109) (a) Liptrot, D. J.; Hill, M. S.; Mahon, M. F.; MacDougall, D. J. *Chem.—Eur. J.* **2010**, *16*, 8508. (b) Spielmann, J.; Bolte, M.; Harder, S. *Chem. Commun.* **2009**, *45*, 6934. (c) Spielmann, J.; Harder, S. *J. Am. Chem. Soc.* **2009**, *131*, 5064.

- (110) Candau, F.; Francois, J.; Benoit, H. *Polymer* **1974**, *15*, 626.
(111) Amoureux, J.-P.; Fernandez, C.; Steuernagel, S. *J. Magn. Reson.* **1996**, *A123*, 116.
(112) Herreros, B.; Metz, A. W.; Harbison, G. S. *Solid State Nucl. Magn. Reson.* **2000**, *16*, 141.

connected to a digital manometer under nitrogen, the system was sealed, and the initial pressure was recorded. At $t_0 = 0$, the contents of the two halves of the Λ -shaped flask were mixed and the pressure monitored continuously. At the intended conversion, the reaction mixture was drawn into a syringe and precipitated within 10 s into hexanes (40 mL) at -78°C . After an additional 30 min, the hexanes were removed at this temperature using a filter cannula and the remaining white solid dissolved in the GPC solvent and was analyzed immediately.

(4) General Procedure for the Polymerization Reactions To Form **8a.** In a 10 mL Schlenk tube *N*-methylamine-borane adduct **7** (224 mg, 5.00 mmol) was dissolved for 15 min in 60% of the total amount of the respective solvent. A solution of the catalyst at the correct amount in the respective solvent (40% of the total amount of the reaction) was made up in a syringe in the glovebox, which was capped with a rubber stopper and transferred out of the glovebox. The Schlenk flask was attached to the nitrogen line, and the catalyst was added quickly. In some cases, complete solubility could not be obtained, but rapid addition of the suspension should have resulted in the transfer of almost all of the catalyst to the reaction mixture. The reactions were allowed to proceed for a set amount of time. In the case of the variation of catalyst loading, solvent, and concentration, the solvent was removed and the residue was analyzed directly by NMR spectroscopy and GPC. In the case of the use of different catalysts, the reaction mixtures were purified by precipitation into hexane at -78°C .

(5) Procedure for the Polymerization with the Morris Catalyst (Fagnou's Catalyst) (10**).** In a 10 mL Schlenk tube *N*-methylamine-borane adduct **7** (224 mg, 5.00 mmol) was dissolved for 15 min in 3.5 mL of THF. This reaction mixture was cooled to -20°C , which led to some precipitation of the amine-borane. In the glovebox, a solution of KO^t-Bu (50 mg, 0.45 mmol) in THF (0.3 mL) was added to the Morris catalyst (dichlorobis[2-(di-*i*-propylphosphino)ethylamine]ruthenium(II) **10**, 14.0 mg, 0.015 mmol, 0.3 mol %). From this stock solution, 0.15 mL was transferred into a syringe, which was capped with a rubber stopper and transferred out of the glovebox and added to the suspension of the amine-borane. After 15 min at -20°C , the reaction mixture was warmed to -10°C and allowed to stir for another 30 min. The mixture was then diluted with 5 mL of THF and purified by precipitation into hexane at -78°C . The solvent was removed from the polymer (off-white powder, 92%) by filtration followed by drying under vacuum.

(6) Synthetic Details and Analytical Data. (a) Poly(*N*-methylaminoborane) **8a.** The synthesis of this material is described as a representative example. *N*-Methylamine-borane adduct **7** (224 mg, 5.00 mmol) was suspended in THF (0.3 mL) and cooled to 0°C . Then the catalyst **5** (9.0 mg, $15\ \mu\text{mol}$, 0.3 mol %) was added as a solution in THF (0.2 mL). Immediate bubbling ensued. After 2 min at this temperature, the cooling bath was removed and the reaction mixture was allowed to stir for 20 min to 1 h at 20°C . Then THF (3 mL) was added, and the reaction mixture precipitated into *n*-butane (approx 12 mL) at -78°C . The mixture was filtered in order to remove *n*-butane at low temperature giving the polymer as a white powder, which was dried overnight under vacuum (60%, $m = 129$ mg, corrected for residual THF = 10% i.e. 6 mol %). Evaporation of the filtrate left a reddish-brown residue that was still catalytically active when treated with a solution of *N*-methylamine-borane in THF.

The polymer can also be purified by precipitation into hexanes at -78°C .

^1H NMR (400 MHz, CDCl_3): $\delta = 2.75$ (1H, NH), 2.18 (3H, CH_3), 1.68 (2H, BH_2) ppm; $^{11}\text{B}\{^1\text{H}\}$ NMR (160 MHz, CDCl_3): -6.5 ppm; ^{13}C NMR (100 MHz, CDCl_3): $\delta = 36.9$ (br), 35.9 ppm; FT-IR: $\tilde{\nu} = 3256$ (N–H), 2985 (C–H), 2366 (B–H) cm^{-1} . Elemental analysis calculated for CH_6NB , corrected for 10% (by wt), 6 mol % of THF detected by NMR: C, 31.9; H, 13.9; N, 29.4. Found: C, 30.5; H, 13.8; N, 28.2. GPC $M_w = 160\ 000$, PDI 2.9 (THF with 0.1 w/w% *n*-Bu₄NBr); DLS (THF) $R_H = 3$ nm; TGA:

Major decomposition temperature: ca. 180°C (inflection point ca. 160°C), ceramic yield: 25% at 600°C .

(b) Key Characterization Data for **8b–8d.** The synthesis of **8b–8d** was achieved in an analogous manner to **8a** using catalyst **5**. However, in the case of **8b** a mixture of **7** and **4** in THF in a 3:1 ratio was used, in the case of **8c** a mixture of **7** and **4** in THF in a 1:1 ratio was used, and in the case of **8d** a more dilute solution (0.5 M in THF) of **4** was used. All of the data below are from samples prepared with **5** as the catalyst.

8b. White powder; ^1H NMR (400 MHz, CDCl_3): $\delta = 3.5$ – 2.39 (m, 5H, 3 NH, $\text{N}'\text{H}_2$), 2.20 (s, 9H, 3 CH_3), 2.05–1.00 ppm (m, 8H, BH_2 B' H_2); $^{11}\text{B}\{^1\text{H}\}$ NMR (160 MHz, CDCl_3): -9.0 ppm; ^{13}C NMR (100 MHz, CDCl_3): $\delta = 35.9$ (br), 35.8 ppm; FT-IR: $\tilde{\nu} = 3256$ (N–H), 2985 (C–H), 2366 (B–H) cm^{-1} . Elemental analysis calculated for $\text{C}_3\text{H}_2\text{N}_4\text{B}_4$, corrected for 12% (by wt) of THF: C, 28.1; H, 13.0; N, 31.3. Found: C, 28.1; H, 13.2; N, 31.2. GPC $M_w = 156\ 000$, PDI 11.0 (THF with 0.1 w/w% *n*-Bu₄NBr); DLS (THF) $R_H = 3$ nm.

8c. White powder; ^1H NMR (400 MHz, $\text{CDCl}_3/\text{DMSO}-d_6$ 1/1): $\delta = 2.71$ – 2.10 (m, 3H, NH, $\text{N}'\text{H}_2$), 1.53 (s, 3H, CH_3), 1.46– 0.50 (m, 4H, BH_2 , B' H_2); $^{11}\text{B}\{^1\text{H}\}$ NMR (160 MHz, CDCl_3): -11.0 ppm; ^{13}C NMR (100 MHz, $\text{CDCl}_3/\text{DMSO}-d_6$ 1/1): $\delta = 34.7$ (br) ppm; FT-IR: $\tilde{\nu} = 3252$ (N–H), 2984 (C–H), 2366 (B–H) cm^{-1} . Elemental analysis calculated for $\text{CH}_{10}\text{N}_2\text{B}_2$, corrected for 15% (by wt) of THF: C, 24.2; H, 13.6; N, 32.2. Found: C, 23.9; H, 13.9; N, 33.5. GPC $M_w = 47\ 000$, PDI 3.9 (THF with 0.1 w/w% *n*-Bu₄NBr); DLS (DMSO) $R_H = 3$ nm the polymer was stable in DMSO by ^{11}B NMR over 24 h under an atmosphere of N_2 .

8d. Insoluble white powder. FT-IR: $\tilde{\nu} = 3299$, 3248 (N–H), 2380, 2312 (B–H) cm^{-1} . Elemental analysis calculated for H_4NB : N, 48.6; H, 14.0. Found: N, 44.0; H, 13.1; C, 4.9. The C presumably arises from residual solvent. TGA: Major decomposition temperature: 220°C (inflection point 200°C), ceramic yield: ca. 40% at 600°C .

WAXS (wide-angle X-ray scattering): major *d*-spacing $3.82\ \text{\AA}$.¹⁰¹

(7) Concentration Dependent DLS and GPC Studies. DLS and GPC studies as shown in section 2 of the Supporting Information. A stock solution of **8a** (4.0 mg/mL) in THF or salt-THF (0.1 w/w% *n*-Bu₄NBr) was prepared in the glovebox. Samples were filtered through a $0.2\ \mu\text{m}$ filter prior to data collection which took ca. 2 h in the case of DLS and 90 min in the case of GPC. Experiments run at 2 and 0.4 mg/mL were achieved by dilution of the 4 mg/mL stock solution in the appropriate solvent, followed by filtration through a $0.2\ \mu\text{m}$ filter.

DLS studies comparing **8a** and a commercial sample of PMMA: Solutions of **8a** or PMMA were prepared in various solvents (THF, THF with 0.1 w/w% *n*-Bu₄NBr, or DMSO) in different concentrations (0.4, 2, 4 mg/mL) in the glovebox by adding the appropriate amount of solvent to an exactly weighed sample. The samples were allowed to stir for 12 and 24 h and were filtered through a $0.2\ \mu\text{m}$ filter prior to data collection.

Acknowledgment. A.S., M.E.S., and A.P.M.R. acknowledge the EPSRC for funding. I.M. thanks the E.U. for a Marie Curie Chair and the Royal Society for a Wolfson Research Merit Award. S.S. and J. S. a. d. G. thank the DFG (Emmy-Nöther Programm, SCHN950/2-1 and SCHM1570/2-1, respectively), and A.F. thanks the Elitenetzwerk Bayern for funding. We thank Mr. Duncan Tarling for the design and engineering of the Λ -shaped flask. We thank the reviewers for helpful comments.

Supporting Information Available: General characterization of **8a** (NMR, IR, GPC, MS, TGA, WAXS, DLS); individual results for the polymerization reactions, experimental setups, pressure–time profiles for the manometric measurements. This material is available free of charge via the Internet at <http://pubs.acs.org>.

JA104607Y